Zoologischer Anzeiger 252 (2013) 246–268

Contents lists available at SciVerse ScienceDirect

Zoologischer Anzeiger

journal homepage: www.elsevier.de/jcz

Zoologischer Anzeiger

Comparative molecular and morphological characterisations in the nematode genus *Rotylenchus*: *Rotylenchus paravitis* n. sp., an example of cryptic speciation

Carolina Cantalapiedra-Navarrete[a], Juan A. Navas-Cortés[a], Gracia Liébanas[b], Nicola Vovlas[c], Sergei A. Subbotin[d,e], Juan E. Palomares-Rius[a], Pablo Castillo[a,*]

[a] *Institute for Sustainable Agriculture (IAS), Spanish National Research Council (CSIC), Alameda del Obispo s/n, Apdo. 4084, 14080 Córdoba, Campus de Excelencia Internacional Agroalimentario, ceiA3, Spain*
[b] *Department of Animal Biology, Vegetal Biology and Ecology, University of Jaén, Campus 'Las Lagunillas' s/n, Edificio B3, 23071 Jaén, Spain*
[c] *Istituto per la Protezione delle Piante, UOS-Bari, Consiglio Nazionale delle Richerche (C.N.R.), Via Amendola 122/D, 70126 Bari, Italy*
[d] *Plant Pest Diagnostic Center, California Department of Food and Agriculture, 3294 Meadowview Road, Sacramento, CA 95832-1448, USA*
[e] *Center of Parasitology of A.N. Severtsov Institute of Ecology and Evolution of the Russian Academy of Sciences, Leninskii Prospect 33, Moscow 117071, Russia*

ARTICLE INFO

Article history:
Received 5 May 2012
Received in revised form 23 July 2012
Accepted 6 August 2012
Available online 19 September 2012
Corresponding Editor: Martin V. Sørensen.

Keywords:
Nematoda
New species
Phylogeny
Spiral nematodes
Taxonomy

ABSTRACT

The nematode *Rotylenchus paravitis* n. sp. infesting roots of commercial sunflowers in southern Spain is described. The new species is characterised by a truncate lip region with 7–9 annuli and continuous with the body contour, lateral fields areolated at pharyngeal region only, body without longitudinal striations, stylet length of 44–50 μm, vulva position at 43–54%, tail rounded to hemispherical with 12–18 annuli. A comparative phenetic study based on a multivariate principal component analysis was developed to determine potential species discrimination. The degree of variation for most characters among specimens of *Rotylenchus paravitis* n. sp. and *R. vitis* was comparable to that observed among specimens belonging to each of the two studied populations of *R. robustus* from Spain and USA. Molecular comparison of the partial 18S, D2-D3 expansion segments of 28S-rRNA, ITS1-rRNA, partial *COI* and *hsp90* from *R. paravitis* n. sp. and *R. vitis*, and other species in the genus, clearly supports the proposal of *R. paravitis* n. sp. as a new species. Consequently, *R. paravitis* n. sp. should be considered as an example of cryptic speciation within the genus *Rotylenchus*. PCR-ITS-RFLP was provided for diagnostics of *R. paravitis* n. sp. and PCR with specific primers were also developed for diagnostics of this new species, *R. vitis* and *R. robustus*. The results of the phylogenetic analysis based on the sequences of the D2-D3 expansion regions of the 28S, ITS1-rRNA genes, and the partial *COI*, have proven to be a powerful tool for providing accurate species identification and assessing phylogenetic relationships within the genus *Rotylenchus*. Phylogenetic testing of D2-D3 expansion segments of 28S-rRNA gene sequences did not refute the monophyly of the genera *Rotylenchus*, *Helicotylenchus*, *Hoplolaimus*, based on tree topologies and the Shimodaira–Hasegawa test even with the split in several clades for some of the genera.

© 2012 Published by Elsevier GmbH.

1. Introduction

The genus *Rotylenchus* Filipjev, 1936 belongs to Hoplolaimidae Filipjev, 1934, a family which also contains agricultural and economically important genera such as *Helicotylenchus* Steiner, 1945, *Hoplolaimus* von Daday, 1905, *Rotylenchulus* Linford and Oliveira, 1940 and *Scutellonema* Andrássy, 1958. This genus tends to be greatly conserved in gross morphology which makes species identification a very difficult task. More than 95 valid species have been recognised in this genus, which confirms the previously mentioned difficulty for identification (Castillo and Vovlas, 2005; Atighi et al., 2011; Cantalapiedra-Navarrete et al., 2012). All the known *Rotylenchus* spp. are obligate plant parasites of a wide range of wild and cultivated plants and are closely associated with plant roots. They are migratory ectoparasites and browse on the surface of roots. As migratory ectoparasites do not enter the plant root, the damage they cause is usually limited to necrosis of those cells penetrated by stylet.

The large number of species within the genus *Rotylenchus* complicates the identification process and has required the construction of tabular and dichotomous keys, based on a combination of major and supplementary characters, to enable pragmatic morphological identification (Castillo and Vovlas, 2005). Recently, DNA-based approaches have been successfully used for the molecular diagnostics of *Rotylenchus* (Vovlas et al., 2008; Atighi et al., 2011; Cantalapiedra-Navarrete et al., 2012). Phylogenetic studies within

* Corresponding author. Fax: +34 957499252.
E-mail address: p.castillo@csic.es (P. Castillo).

0044-5231/$ – see front matter © 2012 Published by Elsevier GmbH.
http://dx.doi.org/10.1016/j.jcz.2012.08.002

Rotylenchus have been carried out based on the D2-D3 expansion regions of the 28S and ITS rRNA gene, providing initial insight towards resolving phylogenetic relationships among *Rotylenchus*, and demonstrating paraphyly of the genus in the majority rule consensus trees within Hoplolaimidae (Subbotin et al., 2007; Vovlas et al., 2008; Cantalapiedra-Navarrete et al., 2012). Molecular analysis of D2-D3 sequences also revealed several *Rotylenchus* species with almost identical sequences, *i.e. Rotylenchus goodeyi* Loof and Oostenbrink, 1958, *Rotylenchus incultus* Sher, 1965, and *Rotylenchus laurentinus* Scognamiglio and Talamé, 1972; or *Rotylenchus robustus* (de Man, 1876) Filipjev, 1936 and *Rotylenchus uniformis* (Thorne, 1949) Loof and Oostenbrink, 1958 (Vovlas et al., 2008). Mitochondrial DNA (mtDNA), particularly the protein-coding mitochondrial gene, cytochrome c oxidase subunit 1 (*COI*), has proven to be a powerful tool for providing accurate species identification and assessing phylogenetic patterns across the animal kingdom, including plant-parasitic and free-living nematodes (Hugall et al., 1994; Derycke et al., 2010; Gutiérrez-Gutiérrez et al., 2011). Similarly, the heat-shock protein *hsp90* gene has also been considered to be a useful molecular marker for species identification or phylogenetic analysis of plant-parasitic nematode species (Skantar and Carta, 2004; Madani et al., 2011). Consequently, both markers may be valuable tools for diagnostics as well as for clarifying phylogenetic relationships in those *Rotylenchus* species with almost identical D2-D3, although no information of these markers is available in this genus and so they need to be developed. Also, molecular techniques have recently shown that many presumed monospecific species are in fact siblings or cryptic species (Subbotin et al., 2003; Vovlas et al., 2008; Gutiérrez-Gutiérrez et al., 2010). Consequently, the nematode species concept should be based on principles of polyphasic taxonomy, which assembles and assimilates all available data and information (phenotypic, morphometric, genotypic and phylogenetic) used for delimiting taxa at all levels (Subbotin and Moens, 2006; Vovlas et al., 2008).

Nematode surveys in agricultural and natural environments in Southern Spain revealed low to moderate soil infestations by two amphimictic populations of *Rotylenchus* species. Preliminary morphological observations indicated that these species appeared to be morphologically similar to *Rotylenchus robustus* (de Man, 1876) Filipjev, 1936, and *Rotylenchus vitis* Cantalapiedra-Navarrete, Liébanas, Archidona-Yuste, Palomares-Rius and Castillo, 2012. Detailed observations using light and scanning electron microscopy (SEM), and molecular characterisation analyses, indicated that these specimens should be assigned to *R. robustus* and to a new species showing close morphological and morphometric resemblance with *R. vitis*, but clearly differentiated by molecular analyses, being considered as an example of cryptic species within the genus *Rotylenchus* (*i.e.* species genetically distinct but sharing common morphological diagnostic characters). In addition, several *Rotylenchus* populations from Australia and USA were collected from natural and cultivated areas to carry out a morphological characterisation combined with molecular analyses which may clarify the phylogeny of the genus.

Therefore, the objectives of this study were: (i) to conduct a comparative phenetic study of the Spanish species resembling *R. vitis* with holotype and paratypes of *R. vitis* of the nematode collection from IAS-CSIC, Córdoba, Spain, as well as two populations of *R. robustus* from Spain and USA, using the most useful diagnostic morphological and morphometric characters for *Rotylenchus* species based on a multivariate principal component analysis; (ii) to verify the taxonomic status of this species close to *R. vitis*, which is described herein as *Rotylenchus paravitis* n. sp., as well as other species from Australia, Spain and USA, conducting detailed morphometric and molecular studies of these *Rotylenchus* species; (iii) to determine the molecular phylogenetic affinities of *R. paravitis* n. sp. and other known *Rotylenchus* species identified in Australia, Spain and USA with closely related species using the rRNA gene sequences (D2-D3 of 28S and ITS1-rRNA), the partial sequences of mitochondrial gene *COI*, and heat shock protein (*hsp90*) gen; and (iv) to provide PCR-ITS-RFLP for *R. paravitis* n. sp. and develop PCR with species specific primers for diagnostics of *R. paravitis* n. sp., *R. vitis* and *R. robustus*.

2. Materials and methods

2.1. Nematode populations

Nematodes of *R. paravitis* n. sp. used in this study were obtained from the rhizosphere of sunflower plants in Jerez de la Frontera (Cádiz province), southern Spain (36°46′28.85″N latitude, 6°15′26.27″W longitude) at an altitude of 16 m a.s.l., and were collected with a shovel from the upper 30 cm of soil on May 2011 by J. Martin-Barbarroja and G. León-Ropero (IAS-CSIC). In addition, Spanish and American populations of *R. robustus* from stone pine in Lucena del Puerto (Huelva province, southern Spain) and grasses in Tomales, California (USA), respectively, a population of *Rotylenchus brevicaudatus* Colbran, 1962 from grasses in Brisbane (Australia), and American populations of *Rotylenchus buxophilus* Golden, 1956, and *Rotylenchus pumilus* (Perry et al., 1959) Sher, 1961, were collected and studied morphometrically and molecularly. In addition, previously morphologically well-characterised *Rotylenchus* populations (Vovlas et al., 2008) from Italy and Spain (including *Rotylenchus cazorlaensis* Castillo and Gómez Barcina, 1987, *Rotylenchus eximius* Siddiqi 1964, *Rotylenchus jaeni* Vovlas, Subbotin, Troccoli and Castillo, 2008, *R. laurentinus*, and *Rotylenchus magnus* Zancada, 1985) were collected to carry out molecular analyses of the partial *COI* sequences which may clarify the phylogeny of the genus. For molecular analyses, a list of studied *Rotylenchus* species and populations is given in Table 1. The nematodes were extracted from rhizosphere soil samples by the centrifugal-flotation method (Coolen, 1979).

Specimens to be observed under light microscopy (LM) were killed by gentle heat, fixed in a solution of 4% formaldehyde + 1% propionic acid and processed to pure glycerin using De Grisse's (1969) method. Specimens were examined using a Zeiss III compound microscope with Nomarski differential interference contrast at up to 1000× magnification. Measurements were done using a *camera lucida* attached to this microscope. For line drawing, hand-made pictures were scanned and imported to CorelDraw software version 12 and redrawn. LM micrographs were based on live specimens for the Spanish population (Fig. 3), and glycerine-mounted specimens for the American populations (Figs. 5–7).

For SEM studies, fixed specimens were dehydrated in a graded ethanol series, critical point dried, sputter-coated with gold and observed with a JEOL JSM-5800 microscope (Abolafia et al., 2002).

2.2. Multivariate principal component analysis

A multivariate principal component analysis was performed on *R. vitis*, *R. paravitis* n. sp., as well as two populations of *R. robustus* from Spain and USA in order to determine the morphometric discrimination among species. The analyses were based upon the following characters: body length (*L*), lip width, lip height, number of lip annuli, stylet length, stylet-conus length, knobs width, dorsal gland orifice (D.G.O.), anterior end to beginning of median pharyngeal bulb distance, anterior end to centre of median pharyngeal bulb distance, total pharyngeal length, anterior end to pharyngo-intestinal junction distance, anterior end, maximum body width, pharyngeal overlapping, cuticle tail tip width, vulva position (*V*), anterior and posterior gonads, female tail length, anal body width, number of female tail annuli, phasmid to terminus

Table 1
Rotylenchus species and populations used and sequenced in the present study.[a]

Species	Locality	Host	D2-D3	ITS1/ITS1-5.8S-ITS2	18S	*COI*
R. agnetis	Potenza, Italy	*Ruscus aculeatus* (Butcher's broom)	EU280795	–	–	–
R. brevicaudatus	Brisbane, Australia	Grasses	**JX015419** **JX015420**	**JX015430** **JX015431**	–	–
R. brevicaudatus	Republic of China	–	–	–	DQ309587	–
R. buxophilus	Napa County, California, USA	Unknown	**JX015421**	**JX015432** **JX015433**	–	**JX015398**
R. buxophilus	Arkansas, USA	–	FJ485646, FJ485647	–	–	–
R. cazorlaensis	Cazorla, Spain	*Quercus faginea* (Portuguese oak)	EU280793	EU373668, EU373669	EU373668	**JX015399** **JX015400**
R. cazorlaensis	Cazorla, Spain	*Quercus rotundifolia* (oak)	EU280792	EU373670, EU373671	–	–
R. conicaudatus	Mazandaran, Iran	Grasses	HQ700698	HQ700700	–	–
R. eximius	Brindisi, Italy	*Pistacia lentiscus* (lentisc)	EU280794	EU373663	–	**JX015401** **JX015402**
R. eximius[b]	Huelva, Spain	*Olea europaea* subsp. *silvestris* (wild olive)	DQ328741	EU373664	**JX015427**	
R. goodeyi	Vejer, Spain	*Olea europaea* subsp. *silvestris* (wild olive)	DQ328756	–	–	–
R. incultus	Niebla, Spain	*Vitis vinifera* (grapevine)	EU280796	EU373673	–	**JX015403**
R. incultus	Bollullos, Spain	*Vitis vinifera* (grapevine)	EU280797	EU373672	–	–
R. iranicus	Mazandaran, Iran	*Fagus orientalis* (beech tree)	HQ700698	HQ700699	–	–
R. jaeni[b]	Santa Elena, Spain	*Quercus suber* (cork tree)	EU280791	EU373661, EU373662	**JX015428**	**JX015404**
R. laurentinus	Torre Canne, Italy	*Pistacia lentiscus* (lentisc)	DQ328757	–	–	**JX015405** **JX015406** **JX015407**
R. laurentinus	Zahara, Spain	*Pistacia lentiscus* (lentisc)	EU280798	EU373666	EU373667	–
R. magnus	Arévalo, Spain	*Ilex aquifolium* (holly)	EU280789	EU373660, EU373676	–	**JX015408** **JX015409** **JX015410**
R. magnus	Lubia, Spain	*Quercus robur* (pedunculate oak)	EU280790	EU373659, EU373665		–
R. montanus	Trentino, Italy	*Malus domestica* (apple)	DQ328743	EU280800, EU280801	–	–
***R. paravitis* n. sp.**[b]	Jerez, Spain	*Helianthus annuus* (sunflower)	**JX015422**	**JX015434**	**JX015429**	**JX015415** **JX015416**
R. pumilus	Santa Clara County, California, USA	*Urtica* sp.	**JX015423**	**JX015435** **JX015436**	–	–
R. robustus[b]	Lucena del Puerto, Spain	*Pinus pinea* (stone pine)	**JX015424**	**JX015437**	–	**JX015413**
R. robustus	Bonares, Spain	*Pinus pinea* (stone pine)	–	–		**JX015414**
R. robustus	Marin County, California, USA	Grasses	**JX015425**	**JX015438**	–	–
R. robustus	Tomales. California, USA	Grasses	**JX015426**	**JX015439** **JX015440**	–	**JX015411** **JX015412**
R. robustus	Michigan, USA	Unknown	EU280788	–	–	–
R. uniformis	Bruges, Belgium	Unknown	DQ328735, DQ328736	–	–	–
R. uniformis	Ghent, Belgium	Unknown	DQ328738	–	–	–
R. uniformis	Poppel, Belgium	Unknown	DQ328739, DQ328740	–	–	–
R. uniformis	Elst, The Netherlands	Unknown	DQ328737	–	–	–
R. unisexus	Seville, Spain	*Citrus aurantium* (citrus)	EU280799	EU373674, EU373675	–	–
R. vitis[b]	Montemayor, Spain	*Vitis vinifera* (grapevine)	JN032581	JN032582	JN032583	**JX015417** **JX015418**
Rotylenchus sp.	Moscow, Russia	Unknown	DQ328742	EU280802	–	–

[a] Newly sequenced samples are indicated by bold font.
[b] *hsp90* gene sequence: **JX015395** for *R. eximius*, **JX015396** for *R. jaeni*, **JX015393** for *R. paravitis* n. sp., **JX015397** for *R. robustus* (Lucena del Puerto), and **JX015394** for *R. vitis*.

distance, phasmid to anus distance, number of annuli between phasmid and anus, and the de Man ratios a, b, b', c, and c', G_1, G_2 and O (Siddiqi, 2000; Table 2).

Principal component analysis was performed with the PRINCOMP procedure of SAS (Statistical Analysis System, version 9.2; SAS Institute Inc., Cary, NC, USA). This analysis produced a set of variables (principal components) that were linear combinations of the original variables. The new variables (principal components) were independent of each other and ranked according to the amount of variation accounted for.

2.3. DNA extraction, PCR and sequencing

Nematode DNA from *R. paravitis* n. sp. and other studied *Rotylenchus* species was extracted from single individuals using proteinase K as described by Castillo et al. (2003). Detailed protocols

Table 2
Eigenvector and eigenvalues of principal components derived from nematode morphometric characters for *Rotylenchus paravitis* n. sp., *R. vitis* and two populations of *R. robustus*.[a]

Character[b]	Principal component			
	PC1	PC2	PC3	PC4
Body length (*L*)	−0.788	−0.154	−0.077	0.467
Lip width	−0.098	−0.256	0.448	−0.003
Lip height	0.237	−0.113	0.088	0.217
Number of lip annuli	−0.660	−0.234	−0.034	0.209
Stylet length	0.307	−0.406	0.390	0.120
Stylet-conus length	0.676	−0.202	0.178	0.096
Knobs width	−0.670	−0.030	0.284	−0.214
Dorsal gland orifice (D.G.O.)	0.727	−0.462	−0.223	0.115
O	0.700	−0.395	−0.328	0.099
Anterior end to beginning of median pharyngeal bulb distance	−0.079	−0.779	0.066	0.285
Anterior end to centre of median pharyngeal bulb distance	−0.062	−0.837	0.037	0.377
Total pharyngeal length	−0.332	−0.727	0.246	0.029
Anterior end to pharyngo-intestinal junction distance	−0.231	−0.634	0.232	0.161
Excretory pore to anterior end (EP)	0.309	−0.592	0.240	0.435
Maximum body width	−0.745	−0.342	0.249	0.059
Pharyngeal overlapping	−0.593	−0.344	−0.038	−0.133
Cuticle tail tip width	−0.755	0.042	0.251	−0.071
Vulva position	0.538	−0.195	−0.003	−0.323
Anterior gonad	−0.561	−0.375	−0.232	−0.567
Posterior gonad	−0.571	−0.382	−0.243	−0.527
G_1	−0.190	−0.315	−0.195	−0.846
G_2	−0.194	−0.334	−0.214	−0.827
Female tail length	0.002	−0.361	−0.831	0.271
Anal body width	−0.592	−0.441	0.113	0.208
Number of female tail annuli	−0.478	−0.256	−0.497	−0.020
Phasmid to terminus distance	−0.839	0.094	−0.322	0.121
Phasmid to anus distance	−0.827	0.182	−0.214	0.097
Number of annuli between phasmid and anus	−0.909	0.190	−0.124	0.045
a	−0.121	0.197	−0.379	0.525
b	−0.777	0.298	−0.105	0.274
b′	−0.572	0.309	−0.258	0.456
c	−0.485	0.207	0.745	0.044
c′	0.332	−0.134	−0.864	0.156
Eigenvalues	9.973	4.823	3.776	3.699
% of total variance	30.22	14.61	11.44	11.21
Cumulative % of total variance	30.22	44.83	56.28	67.49

[a] Based on 21 female specimens of *Rotylenchus vitis* and *R. paravitis* n. sp., respectively, and 12 and nine female specimens of two populations of *R. robustus* from Spain and USA, respectively. Values of morphometric and morphological characters dominating principal components 1–4 (eigenvector >0.63) are underlined.
[b] Morphological and diagnostic characters according to Castillo and Vovlas (2005).

for PCR and sequencing were applied as described by Castillo et al. (2003). The primers used for amplification of D2-D3 regions of 28S, ITS1-rRNA, the partial 18S, the *COI* and *hsp90* gene, as well as those for species specific PCR are listed in Table 3. These sequences were used for molecular species characterisation and phylogenetic analyses.

PCR products were purified after amplification with Geneclean turbo (Q-BIOgene SA, Illkirch Cedex, France) or QIAquick (Qiagen,

Table 3
Primers sets used in the present study.

Primer code	Sequences 5′–3′	Amplified gene	References
TW81	GTTTCCGTAGGTGAACCTGC	ITS-rRNA	Curran et al. (1994)
AB28	ATATGCTTAAGTTCAGCGGGT		
D2A	ACAAGTACCGTGAGGGAAAGTTG	D2-D3 of 28S rRNA	Subbotin et al. (2006)
D3B	TCGGAAGGAACCAGCTACTA		
TW81	GTTTCCGTAGGTGAACCTGC	ITS1-rRNA	Vovlas et al. (2008)
5.8SM5	GGCGCAATGTGCATTCGA		
A	AAAGATTAAGCCATGCATG		
13R	GGGCATCACAGACCTGTTA	18S	Boutsika et al. (2004)
18P-SSU_R_81	TGATCCWKCYGCAGGTTCAC		
JB3	TTTTTTGGGCATCCTGAGGTTTAT	*COI*	Derycke et al. (2010)
JB4	TAAAGAAAGAACATAATGAAAATG		
U831	AAYAARACMAAGCCNTYTGGAC	*hsp90*	Skantar and Carta (2004)
L1110	TCRCARTTVTCCATGATRAAVAC		
TW81	GTTTCCGTAGGTGAACCTGC	ITS-rRNA	This study
R_paravitis	GCTCCATCACGCAGCAGAC		
TW81	GTTTCCGTAGGTGAACCTGC	ITS-rRNA	This study
R_vitis	CTTACGTGTGTGCCAAATAGTG		
TW81	GTTTCCGTAGGTGAACCTGC	ITS-rRNA	This study
R_robustus	GACGTGGACATCATACAGTC		

USA) gel extraction kits, quantified using a Nanodrop spectrophotometer (Nanodrop Technologies, Wilmington, DE, USA) and used for direct sequencing in both directions using the primers referred above. The resulting products were purified and run on a DNA multicapillary sequencer (Model 3130XL genetic analyser; Applied Biosystems, Foster City, CA, USA), using the BigDye Terminator Sequencing Kit v.3.1 (Applied Biosystems, Foster City, CA, USA), at the SCAI, University of Córdoba sequencing facilities (Córdoba, Spain). The newly obtained sequences were submitted to the GenBank database under accession numbers indicated on the phylogenetic trees and Table 1.

2.4. Phylogenetic analysis

D2-D3 expansion segments of 28S, ITS1-rRNA, partial *COI*, the partial 18S, and partial *hsp90* gen newly sequenced and sequences obtained from GenBank were used for phylogenetic reconstruction. Outgroup taxa for D2-D3 expansion regions of 28S-rRNA dataset were chosen according to previous published data (Vovlas et al., 2008). The newly obtained and published sequences for each gene were aligned using ClustalW (Thompson et al., 1997) with default parameters. Sequence alignments were manually edited using BioEdit (Hall, 1999). Phylogenetic analyses of the sequence data sets were performed under maximum likelihood (ML) using PAUP* 4b10 (Swofford, 2003) and Bayesian inference (BI) using MrBayes 3.1.2 (Huelsenbeck and Ronquist, 2001). The best fitting model of DNA evolution was obtained based on the Akaike Information Criterion (AIC) using jModelTest v.0.1.1 (Posada, 2008) with. The Akaike-supported model, the base frequency, the proportion of invariable sites, and the gamma distribution shape parameters and substitution rates in the AIC were then used in phylogenetic analyses. BI analysis under TVM + I + G model for D2-D3 expansion segment of 28S-rRNA; TVM + G for ITS1 region and GTR + I + G for *COI*, TIM1 + I + G for partial 18S, and K80 + G for *hsp90* gene were run with four chains for 5×10^6, 1×10^6, 1×10^6, 1×10^6, and 2×10^6 generations, respectively. The Markov chains were sampled at intervals of 100 generations. Two runs were performed for each analysis. After discarding burn-in samples and evaluating convergence, the remaining samples were retained for further analyses. The topologies were used to generate a 50% majority rule consensus tree. Posterior probabilities (PP) are given on appropriate clades. Trees were visualised using TreeView (Page, 1996). In ML analysis the estimation of the support for each node was obtained by bootstrap analysis with 100 fast-step replicates. In order to test alternative tree topologies by constraining hypothetical monophyletic groups, we performed the Shimodaira–Hasegawa test (SH-test) as implemented in PAUP (Swofford, 2003) and using the RELL option, based on D2-D3 expansion segments of 28S and partial 18S from 37 and 15 selected taxa, respectively: D2-D3 expansion segments of 28S for the genera *Rotylenchus*, *Helicotylenchus*, *Scutellonema*, *Aorolaimus* and *Hoplolaimus*; partial 18S for *Rotylenchus*, *Helicotylenchus* and *Scutellonema*. *Aglenchus agricola* (AY780979, FJ969113), *Coslenchus costatus* (DQ328719, AY284581) and *Basiria gracillis* (DQ328717, EU130839) were used as outgroups in both datasets (Vovlas et al., 2008; Subbotin et al., 2007). Species in datasets including D2-D3 expansion segments of 28S were selected from the clades formed in the previous study of phylogeny of Hoplolaimidae performed by Cantalapiedra-Navarrete et al. (2012). Tests constraining hypothetical groups were performed using ML (Table 8).

2.5. RFLP-ITS-rRNA

Three to seven μl of purified PCR product of the D2-D3 of 28S-rRNA gene for *R. paravitis* n. sp. was digested by one of following restriction enzymes: *Ava*I, *Rsa*I, *BseN*I, *Mva*I or *Hpa*II, in the buffer stipulated by the manufacturer. The digested DNA was run on a 1.4% TAE buffered agarose gel, stained with ethidium bromide, visualised on UV transilluminator and photographed. The exact lengths of each restriction fragment from the PCR products were obtained by a virtual digestion of the sequences using WebCutter 2.0 (www.firstmarket.com/cutter/cut2.html).

2.6. PCR with species specific primers

Species specific primers were developed for several species: *R. paravitis* n. sp., *R. vitis* parasitising grapevine in Spain and the type species of the genus and agricultural important species *R. robustus*. Specific primers were designed based on unique fragments for each species using sequence alignment of ITS-rRNA gene. Several *Rotylenchus* samples were used to test species specific primers. PCR mixture was prepared as described in Tanha Maafi et al. (2003). The universal forward TW81 primer was used in PCR with combinations of the specific reverse *R. paravitis*, *R. vitis* or *R. robustus* primers (Table 3) for diagnostics of *R. paravitis* n. sp., *R. vitis* or *R. robustus*, respectively. The PCR amplification profile consisted of 4 min at 94 °C; 30 cycles of 1 min at 94 °C, 45 s at 57 °C and 45 s at 72 °C, followed by a final step of 10 min at 72 °C. Four μl of the PCR product was run on a 1.4% TAE buffered agarose gel, stained and photographed.

3. Results

3.1. Comparative multivariate analysis of Rotylenchus paravitis n. sp., Rotylenchus vitis, and two populations of Rotylenchus robustus

In the principal component analysis, the first four principal components accounted for 67.5% of the total variance of morphological and morphometric characters of the four *Rotylenchus* populations included in the analysis (Table 2). Table 2 includes the eigenvalues for the first four principal components (PC) that were used to interpret the significance of the PCs. Principal component 1separates *R. vitis* and *R. paravitis* n. sp. specimens from the two populations of *R. robustus*, characterised by smaller values of stylet-conus length, D.G.O, and *O* ratio, and higher values for body size (length and width), knobs width, cuticle tail tip width, phasmid to terminus and anus distances, number of annuli between phasmid and anus, and *b* ratio (Table 2 and Fig. 1), but did not separate *R. vitis* from *R. paravitis* n. sp. Similarly, the stylet conus and orifice of dorsal gland of *R. robustus* specimens were lower than that observed for *R. vitis* and *R. paravitis* n. sp. with no differences between these two species or between the two *R. robustus* populations (Fig. 1A–C).

Principal component 2 is dominated by high negative weights for anterior body end to centre and beginning of median pharyngeal bulb distances, total pharyngeal length and anterior end to pharyngo-intestinal junction distance (Table 2 and Fig. 1A), relating this factor with pharyngeal dimensions. These characters showed a large but similar degree of variation among specimens of the three *Rotylenchus* species in the study (Fig. 1A).

When projected on the plane of PCs 1 and 3, female tail shape and size and *c′* ratio decreased from bottom to top. According to their relative position to y axis in Fig. 1B, specimens of *R. paravitis* n. sp. were characterised by lower values for these two characters when compared to that of *R. vitis*, although some specimens of the two species showed also similar values (Fig. 1B). Similarly, when projected on the plane of PCs 1 and 4, specimens of *R. vitis* tended to have longer gonads than that of *R. paravitis* n. sp. (Fig. 1B and C).

Concerning *R. robustus* populations, a similar range of variation for characters related to PC 3 (Fig. 1B) or PC 4 (Fig. 1C) were observed among specimens of the two *R. robustus* populations.

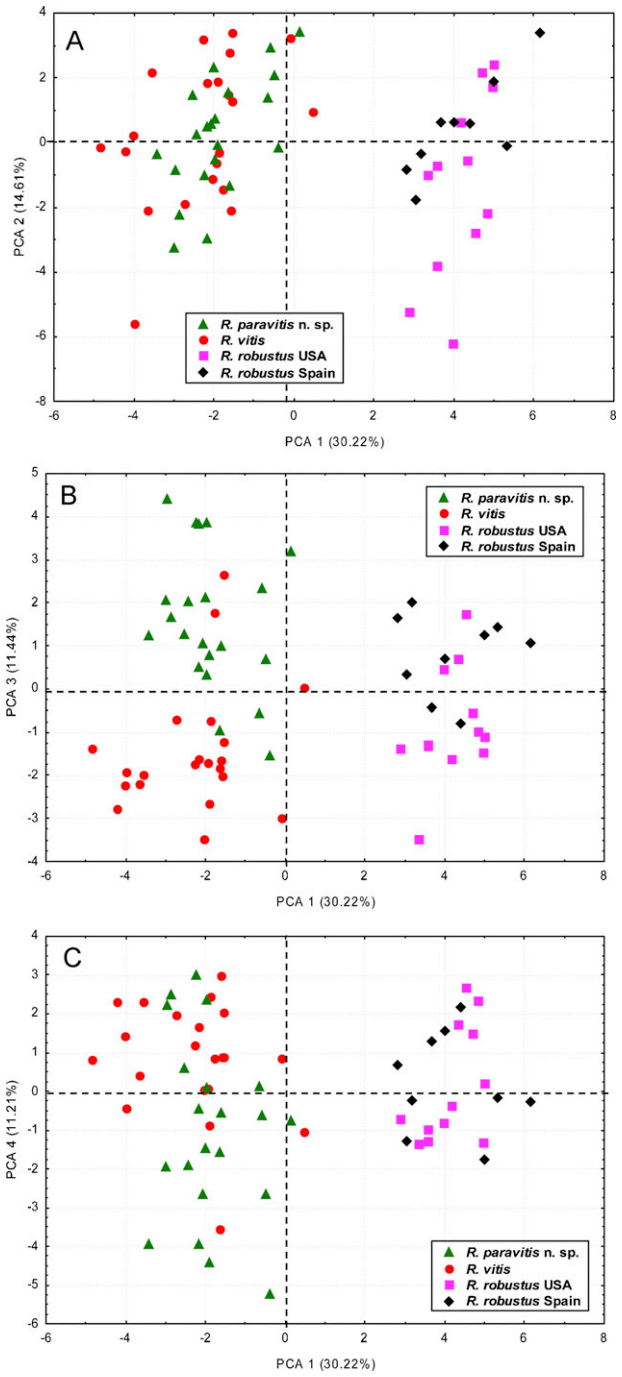

Fig. 1. Principal component (PC) analysis of 33 morphometric characters used to characterise 21 specimens of *Rotylenchus vitis* and *R. paravitis* n. sp., respectively, and 12 and nine specimens of two populations of *R. robustus* from Spain and USA, respectively. Projection of morphometric characters on the plane of PC 1 and 2 (A), 1 and 3 (B), and 1 and 4 (C).

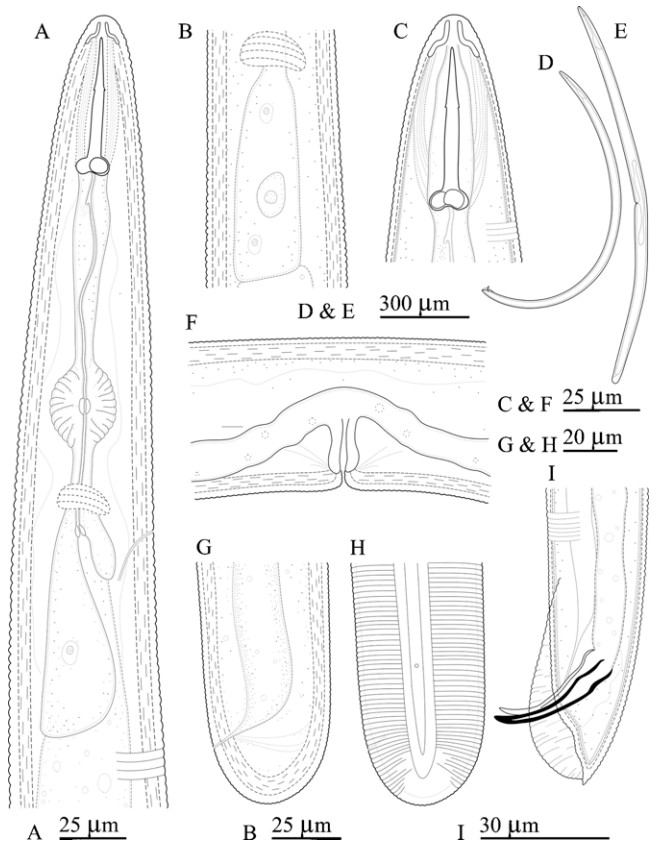

Fig. 2. *Rotylenchus paravitis* n. sp. (A) Female pharyngeal region. (B) Detail of pharyngeal gland. (C) Female anterior body region. (D, E) Male and female habitus. (F) Vulval region. (G, H) Female tail regions. (I) Male tail region.

3.2. Systematics

Family Hoplolaimidae Filipjev, 1934
Rotylenchus Filipjev, 1936.

3.2.1. *Rotylenchus paravitis* n. sp.

Figs. 2–4 and Table 4.

3.2.1.1. Holotype and paratypes. Holotype female, extracted from in a clay soil from the rhizosphere of sunflower (*Helianthus annuus* L.) in Jerez de la Frontera, Cádiz province, southern Spain, by J. Martín-Barbarroja and G. León Ropero, mounted in pure glycerine and deposited in the nematode collection at Institute for Sustainable Agriculture (IAS) of Spanish Council for Scientific Research (CSIC), (collection number IAS-J174-02). Female and male paratypes extracted from the same soil as holotype, and deposited in the Nematode Collection at the Institute for Sustainable Agriculture, CSIC, Córdoba, Spain. Another two female paratypes deposited at each of the following collections: Istituto per la Protezione delle Piante (IPP) of Consiglio Nazionale delle Ricerche (C.N.R.), Sezione di Bari, Bari, Italy; USDA Nematode Collection, Beltsville, MD, USA (collection number G-18577) and WaNeCo, Plant Protection Service, Wageningen, The Netherlands. Specific D2-D3, ITS1, 18S-rRNA, *COI* and *hsp90* sequences are deposited in GenBank with accessions numbers JX015422, JX015434, JX015429, JX015415, JX015416, and JX015393, respectively.

3.2.1.2. Diagnosis. Rotylenchus paravitis n. sp. is a gonochoristic species assigned to the species group having more than six lip annuli, a truncate lip region, female tail usually hemispherical to broadly rounded and stylet more than 35 µm long (Castillo and Vovlas, 2005). It is characterised by a truncate lip region clearly narrowing in the first half, with 7–9 annuli, continuous with body contour, lateral fields areolated at pharyngeal region only, body without longitudinal striations, stylet length of 44–50 µm, vulva position at 43–54%, tail rounded to hemispherical, with 12–18 annuli, and a specific D2-D3, ITS1-rRNA, partial 18S, *COI* and *hsp90* sequences. Intra-specific variability of D2D3 was evaluated by sequencing two specimens showing high similarity (99%), differing in 1/682 nucleotides and showing no indels between them.

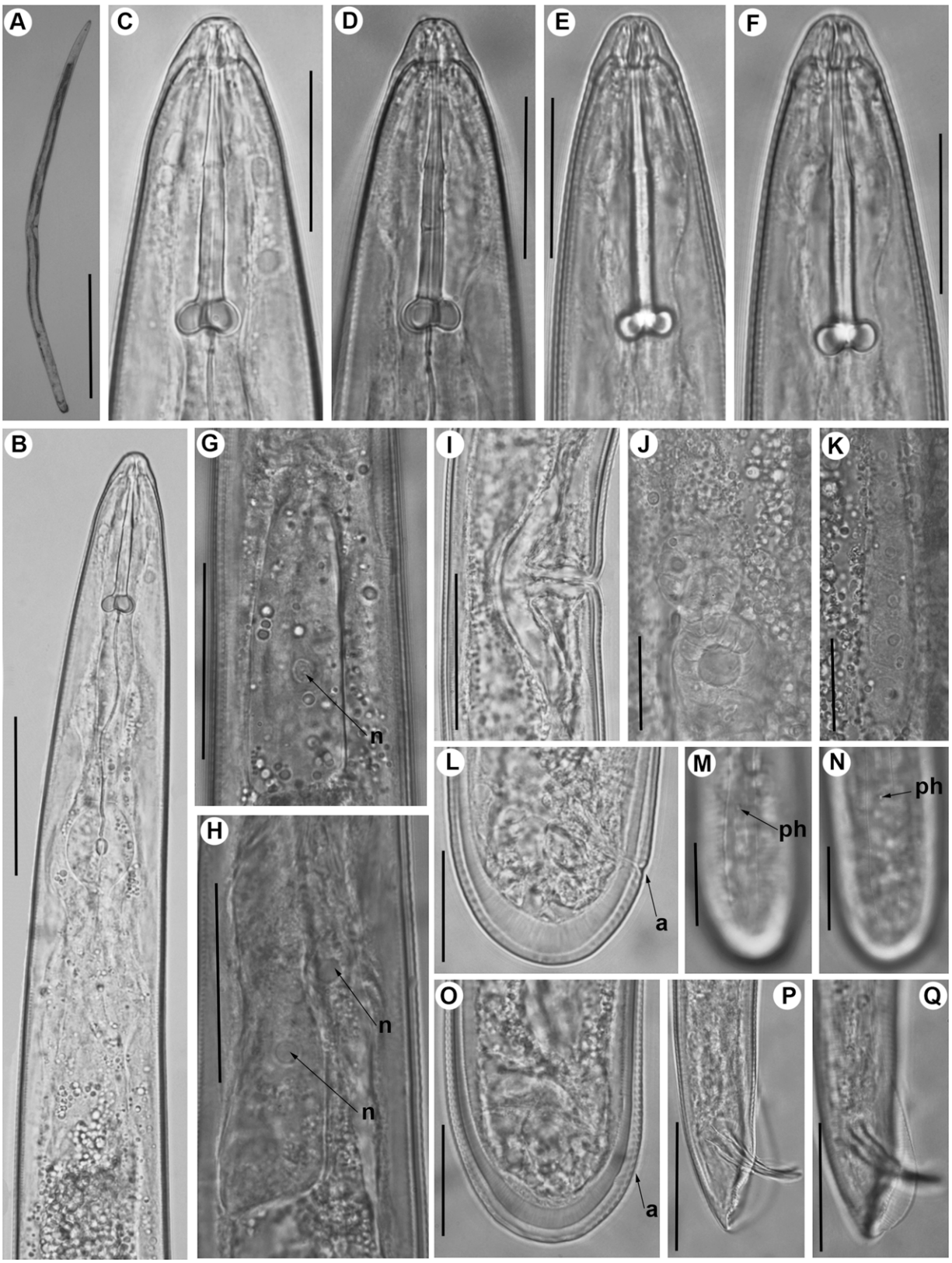

Fig. 3. Light micrographs of *Rotylenchus paravitis* n. sp. (A) Female habitus. (B) Female pharyngeal region. (C–F) Female anterior body region. (G, H) Detail of pharyngeal gland. (I) Vulval region. (J) Detail of spermatheca. (K) Detail of ovary. (L–O) Female tail regions. (P–Q) Male tail region. *Abbreviations*: a: anus; n: gland nucleus; ph: phasmid (scale bars: A: 500 μm; B: 50 μm; C–F: 25 μm; G–I: 50 μm; J–O: 25 μm; P–Q: 50 μm).

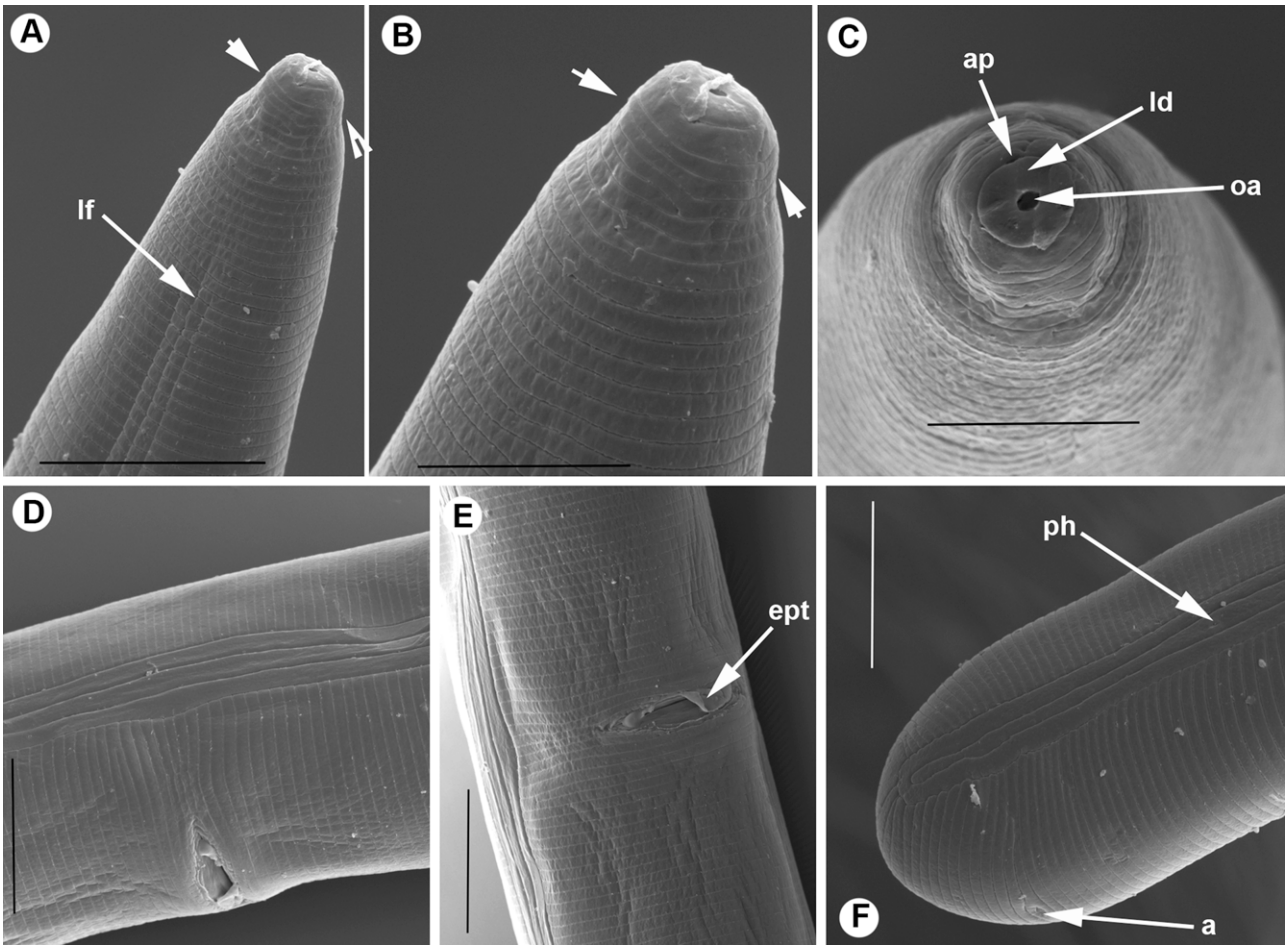

Fig. 4. Scanning electron microscope photographs of *Rotylenchus paravitis* n. sp. (A, B) Female lip region, lateral view, showing anterior narrowing (arrowed) and beginning of lateral fields (lf). (C) *En face* view showing oral aperture (oa), amphid (ap) and labial disc (ld). (D, E) Vulval region showing non-areolated lateral fields and few developed epiptygma (ept). (F) Female tail region showing anus (a) and phasmid (ph) (scale bars: A, D–F = 20 μm; B, C = 10 μm).

3.2.1.3. Description. Female: Body large, habitus slightly curved ventrally to open C-shaped. Lateral fields with four smooth equidistant lines, beginning anteriorly at 12–14th annulus as three lines forming two bands; after 20–23 annuli, central line dividing to form a third band. The three bands are 10.6 ± 0.8 (9.5–12.0) μm wide at mid-body, approximately one-fifth as wide as body diam. Regular areolation of lateral fields (external bands) observed in pharyngeal region. Cuticle 2.0–3.0 μm thick, clearly annulated, annuli 1.5 μm wide at mid-body. Body without longitudinal striations in any region. Labial region truncate, continuous with body, clearly narrowing in the first half, bearing 7–9 narrow annuli which are not divided longitudinally. Labial disc distinct under SEM, but not in lateral view under LM. Oral aperture oval (1.0–1.2 × 0.8–1.0 μm), labial disc oval (4.5–5.0 × 3.5–4.0 μm) bordered by amphidial apertures. Oral disc clearly separated from first annulus of lip region, which is undivided. Labial framework well developed, 5.3 ± 0.4 μm (5–6) long, posterior margin at level of 7th or 9th body annulus. Stylet robust, 3.1–3.8 times longer than labial region diam. Basal knobs slightly flattened posteriorly, 8.0–10.5 μm wide, at level of 25–32nd annulus posterior to labial region. Dorsal pharyngeal gland opening 4.0–7.0 μm posterior to stylet base. Procorpus of pharynx cylindrical, with slight depression just anterior to median bulb, 51.4 ± 5.0 (44–61) μm long. Median pharyngeal bulb well developed, broadly oval, 21–29 × 19–24 μm, occupying 10–12 annuli, valvular apparatus 5.0–6.5 μm long, located at 46.1 ± 3.8 (41–51)% of pharyngeal length. Isthmus 23.4 ± 2.8 (19–28) μm long, encircled by nerve ring at mid-point. Pharyngeal glands sacciform, with three nuclei, overlapping intestine dorsally for 24–52 annuli. Nerve ring enveloping isthmus at middle, at 127 ± 10.8 (113–153) μm from anterior end. Excretory pore usually located near pharyngo-intestinal junction level, but varying from anterior to posterior of pharyngeal-intestinal valve. Hemizonid distinct, located at anterior to excretory pore, extending for *ca* 1.5–2.0 body annuli width, just anterior to excretory pore, rarely posterior. Reproductive system with both genital branches equally developed; anterior branch 315 ± 64.1 (217–416) μm long, posterior branch 300 ± 54.9 (203–369) μm long. Vulva slightly posterior to mid-body, undistinct epiptygma under LM but clearly distinguishable under SEM (Fig. 4D and E). Vagina with internal walls slightly sclerotised, 20.5 (18–24) μm long. Ovaries with a single row of oocytes, spermathecae not functional, without sperm. Phasmids pore-like, 19.1 ± 2.6 (12–24) annuli anterior to level of anus or 24.9 ± 3.9 (15.5–28.0) μm anterior to anus. Tail short, usually hemispherical to broadly rounded, with 12–18 annuli, terminus striated and cuticle at tail tip 8.2 ± 0.6 (7.5–10.0) μm wide.

Male: Very rare, only one specimen detected. Habitus slightly curved ventrally. Morphology similar to that of females, except for the following characters: lip region slightly more elevated in outline, 10.0 μm wide and 5.0 μm high; stylet shorter than that of female; stylet knobs less developed (5.5 μm wide). Testis single, anteriorly outstretched, 494 μm long. Tail conoid, 1.7 times shorter than that of female. Phasmid distinct, situated anteriorly

Table 4
Morphometrics of *Rotylenchus paravitis* n. sp. from the rhizosphere of sunflower (*Helianthus annuus* L.) from Jerez de la Frontera, Cádiz province, southern Spain. All measurements are in μm and in the form: mean ± s.d. (range).[a]

Character	Females		Males
	Holotype	Paratypes	Paratype
n	–	20	1
L	1644	1599 ± 144.1 (1383–1856)	1167
a	35.0	32.1 ± 1.7 (29.3–34.6)	37.6
b	14.7	15.3 ± 0.9 (13.6–17.0)	17.2
b′	7.7	7.6 ± 0.5 (6.7–8.5)	8.7
c	67.1	79.7 ± 15.2 (55.3–104.9)	55.6
c′	0.7	0.6 ± 0.1 (0.4–0.8)	1.2
V or *T*	52.0	51.2 ± 2.7 (43–54)	42
G_1	18	17.0 ± 5.0 (12.6–29.8)	–
G_2	19	16.5 ± 4.2 (12.1–26.7)	–
Stylet	47.5	46.5 ± 1.7 (44.0–50.0)	33.5
Stylet conus	21.5	21.1 ± 1.0 (19.0–22.5)	15.5
D.G.O.	4.0	4.4 ± 0.8 (4.0–7.0)	4.0
O	8.4	9.5 ± 1.6 (8.2–14.6)	11.9
Anterior end to centre of median bulb	112.0	106 ± 6.0 (97–116)	68
Anterior end to excretory pore	151.0	148 ± 11.3 (136–166)	95
Pharynx length	213.0	210 ± 14.6 (195–244)	134
Pharyngeal overlap	60.0	57.7 ± 4.5 (53–67)	47
Max. body diam.	47.0	50.5 ± 4.7 (44–61)	31
Anal body diam.	34.0	36.3 ± 3.5 (30.0–43.0)	18
Tail	24.5	20.8 ± 3.5 (16.0–28.0)	21
Tail annuli	14.0	15.4 ± 1.7 (12–18)	–
Phasmid to terminus	58.0	46.7 ± 4.6 (40.0–54.0)	–
Spicules	–	–	33
Gubernaculum	–	–	13

[a] Abbreviations are defined in Siddiqi (2000).

at anus level. Bursa 54 μm long, completely surrounding tail which is tapering with a rounded-pointed tip. Gubernaculum prominent, with distinct titillae.

3.2.1.4. Type locality. *Rotylenchus paravitis* n. sp. was found in a clay soil from the rhizosphere of sunflower (*Helianthus annuus* L.) in Jerez de la Frontera, Cádiz province, southern Spain.

3.2.1.5. Etymology. The species epithet refers to Gr. prep. *para*, alongside of, resembling; N.L. masc. n. *vitis*, a morphologically close species (*Rotylenchus vitis*).

3.2.2. *Rotylenchus brevicaudatus* Colbran, 1962

Fig. 5 and Table 5.

Female: Habitus spiral. Lip region continuous with body contour, marked by 4 annuli. Lateral fields with four smooth equidistant lines, the three bands are 5.1 ± 0.3 (5.0–5.5) μm wide at mid-body, approximately one-fifth as wide as body diam. Regular areolation of lateral fields (external bands) observed in pharyngeal region. Cuticle 1.5 μm thick, clearly annulated, one annulus 1.5 μm wide at mid-body. Body without longitudinal striations in any region. Stylet moderately robust, 2.3–2.5 times longer than labial region diam. Basal knobs rounded slightly backwards directed, 4.0–4.5 μm wide. Dorsal pharyngeal gland opening 5.0–5.5 μm posterior to stylet base. Procorpus of pharynx cylindrical, with slight depression just anterior to median bulb, 34.8 ± 1.0 (34–36) μm long. Median pharyngeal bulb well developed, broadly oval, 10.0–11.0 × 9.0–10.0 μm, occupying 6–8 annuli, valvular apparatus 2.0–2.5 μm long, located at 55.6 ± 4.1 (51–59)% of pharyngeal length. Isthmus 22.5 ± 1.3 (21–24) μm long, encircled by nerve ring at mid-point. Pharyngeal glands short, with three nuclei, slightly overlapping intestine dorsally for 4–6 annuli. Nerve ring enveloping isthmus at middle, at 81 ± 3.6 (76–84) μm from anterior end. Excretory pore usually located near pharyngo-intestinal junction level. Hemizonid distinct, 2–3 annuli long, located 1–3 annuli anterior to excretory pore, extending for *ca* 1.0–1.5 body annuli width. Reproductive system with both genital branches equally developed; anterior branch 91 ± 18.9 (72–114) μm long, posterior

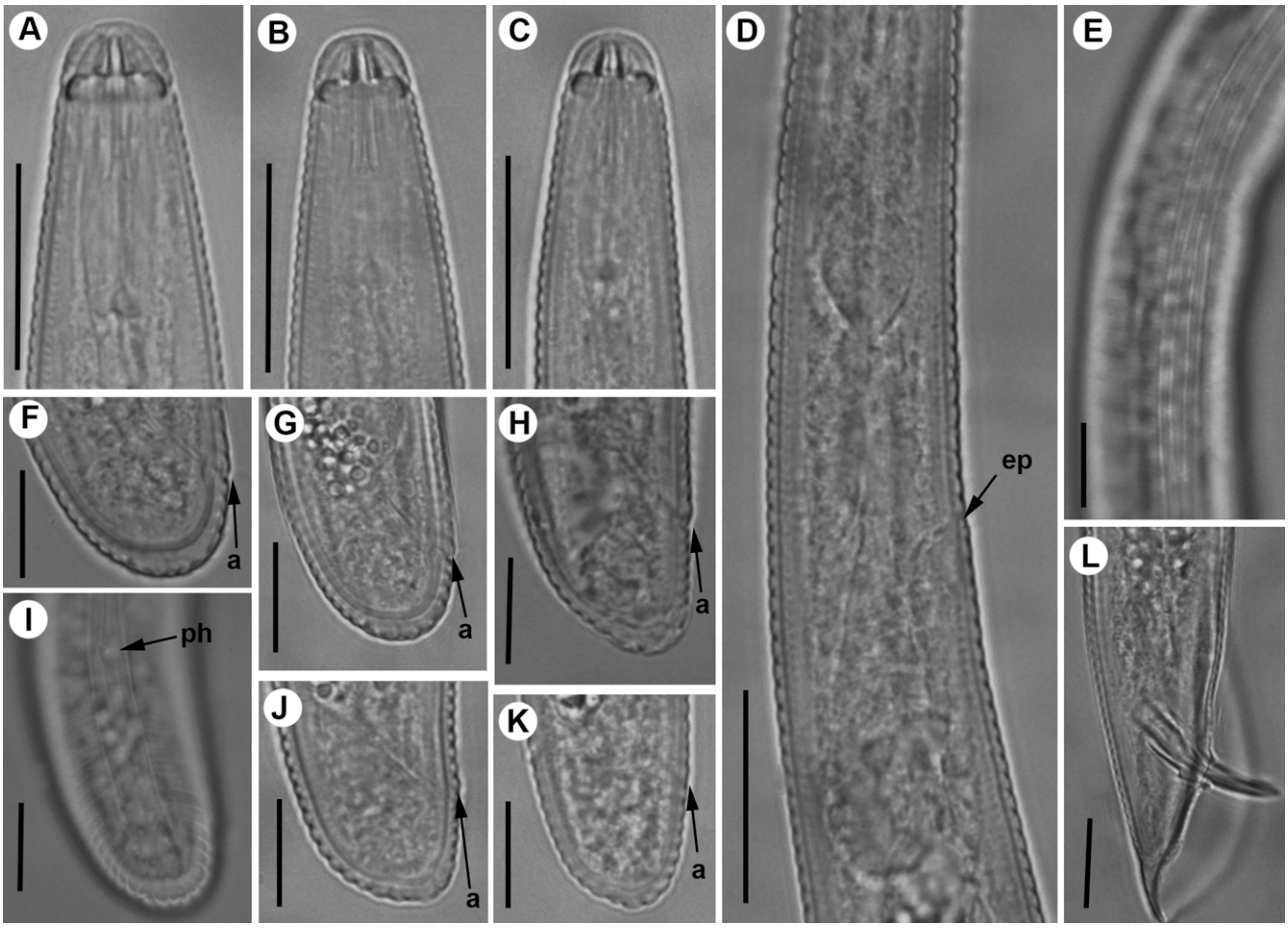

Fig. 5. Light micrographs of *Rotylenchus brevicaudatus* Colbran, 1962 (A–C) Female anterior body region. (D) Detail of pharyngeal region. (E) Lateral fields at mid-body. (F–K) Female tail regions. (L) Male tail region. *Abbreviations*: a: anus; ep: excretory; ph: phasmid (scale bars: A–D: 20 μm; B: 50 μm; E–L: 10 μm).

branch 86 ± 19.3 (67–111) μm long. Vulva clearly posterior to mid-body, without a distinct epiptygma. Vagina with internal walls slightly sclerotised, 10.5 (10.0–11.0) μm long. Ovaries with a single row of oocytes. Phasmids pore-like, 10.0 ± 2.8 (8–14) annuli anterior to level of anus or 13.9 ± 1.9 (12.0–16.5) μm anterior to anus. Tail short, conoid-rounded, terminus hemispherical, coarsely striated and cuticle at tail tip 2.6 ± 0.3 (2.5–3.0) μm wide.

Male: Habitus a closed C shape. Lip region similar than that of female. Bursa crenate, enveloping tail, 43.7 ± 2.4 (41–48) μm. Spicules slightly cephalated and ventrally arcuate. Gubernaculum protrusible. Testis single, outstretched.

3.2.3. *Rotylenchus buxophilus* Golden, 1956

Fig. 6 and Table 5.

Female: Habitus from close C to spiral. Lip region hemispherical, separated from body contour by a slight constriction, marked by 4–5 annuli. Lateral fields with four smooth equidistant lines, the three bands are 7.8 ± 0.6 (7.0–8.5) μm wide at mid-body, approximately one-fifth as wide as body diam. Regular areolation of lateral fields (external bands) observed in pharyngeal region. Cuticle 1.5 μm thick, clearly annulated, annuli 1.0–1.5 μm wide at mid-body. Body without longitudinal striations in any region. Stylet robust, 2.8–3.1 times longer than labial region diam. Basal knobs rounded slightly laterally directed, 6.0–7.5 μm wide. Dorsal pharyngeal gland opening 4.0–5.0 μm posterior to stylet base. Procorpus of pharynx cylindrical, with slight depression just anterior to median bulb, 42.9 ± 1.7 (40–46) μm long.

Median pharyngeal bulb well developed, broadly oval, 15.0–16.0 × 12.0–13.0 μm, occupying 9–11 annuli, valvular apparatus 2.0–2.5 μm long, located at 50.9 ± 1.5 (48–53)% of pharyngeal length. Isthmus 28.5 ± 1.9 (26–32) μm long, encircled by nerve ring at mid-point. Pharyngeal glands forming a compact lobe, with three nuclei, overlapping intestine dorsally. Nerve ring enveloping isthmus at middle, at 105 ± 11.1 (98–126) μm from anterior end. Excretory pore usually located near pharyngo-intestinal junction level. Hemizonid distinct, located 2–3 annuli long, 1–3 annuli anterior to excretory pore. Reproductive system with both genital branches almost equally developed; anterior branch 210 ± 29.3 (171–250) μm long, posterior branch 193 ± 19.3 (158–242) μm long. Vulva clearly posterior to mid-body, without a distinct epiptygma. Vagina with internal walls slightly sclerotised, 13.5 (13.0–14.0) μm long. Ovaries with a single row of oocytes. Phasmids pore-like, 8.2 ± 2.2 (6–11) annuli anterior to level of anus or 10.3 ± 4.4 (6.0–16.0) μm anterior to anus. Tail dorsally convex-conoid-rounded, terminus pointed, striated and cuticle at tail tip 3.2 ± 0.6 (2.5–4.0) μm wide.

3.2.4. *Rotylenchus pumilus* (Perry et al., 1959) Sher, 1961

Fig. 7 and Table 5.

Female: Habitus usually forming a spiral, slightly tapering towards extremities. Lip region hemispherical, continuous with body contour or slightly separated by a depression, marked by 4–5 annuli. Lateral fields with four smooth equidistant lines, the three bands are 8.1 ± 0.2 (8.0–8.5) μm wide at mid-body, approximately one-fourth as wide as body diam. Regular areolation of lateral fields (external bands) observed in pharyngeal region. Cuticle 1.5–2.0 μm thick, clearly annulated, annuli 1.5 μm wide at mid-body. Body without longitudinal striations in any region.

Table 5
Morphometrics of *Rotylenchus brevicaudatus* Colbran, 1962 from grasses (Brisbane, Australia), *Rotylenchus buxophilus* Golden, 1956 from Napa Valley (California, USA), and *Rotylenchus pumilus* (Perry et al., 1959) Sher, 1961 from *Urtica* sp. San Jose park, California, USA. All measurements are in μm and in the form: mean ± s.d. (range).[a]

Character	*R. brevicaudatus*		*R. buxophilus*	*R. pumilus*
	Females	Males	Females	Females
n	4	6	10	6
L	571.8 ± 56.0 (502–618)	565.8 ± 20.1 (533–587)	948 ± 95.0 (829–1142)	825 ± 50.4 (773–906)
a	23.9 ± 1.8 (21.8–25.7)	23.8 ± 0.7 (23.1–24.9)	30.8 ± 2.6 (25.4–28.9)	26.9 ± 1.5 (25.4–28.9)
b	8.9 ± 0.6 (8.2–9.5)	8.8 ± 0.1 (8.5–8.9)	7.3 ± 0.8 (6.4–8.9)	11.1 ± 0.7 (10.3–12.2)
b′	5.3 ± 0.0 (5.3–5.3)	4.8 ± 0.2 (4.5–5.0)	6.1 ± 0.6 (5.4–7.3)	6.5 ± 0.4 (5.9–7.0)
c	54.8 ± 11.0 (41.8–68.7)	34.9 ± 2.0 (32.6–38.1)	37.5 ± 2.9 (33.2–42.0)	46.6 ± 2.9 (42.9–50.2)
c′	0.6 ± 0.1 (0.5–0.7)	1.1 ± 0.01 (1.1–1.2)	1.2 ± 0.1 (1.1–1.5)	0.9 ± 0.1 (0.8–1.0)
V or *T*	56.5 ± 1.3 (55.0–58.0)	46.2 ± 2.9 (42.3–49.7)	55.4 ± 1.8 (54.0–57.0)	56.7 ± 1.8 (54.0–59.0)
G_1	16.0 ± 3.1 (11.7–18.5)	–	21.5 ± 0.7 (15.0–25.9)	19.1 ± 0.7 (18.3–20.1)
G_2	15.0 ± 3.0 (10.8–18.0)	–	19.6 ± 2.7 (16.1–24.0)	17.3 ± 1.5 (14.6–18.8)
Stylet	22.4 ± 1.3 (21.0–24.0)	20.8 ± 0.8 (20.0–22.0)	35.5 ± 1.2 (33.0–37.0)	29.3 ± 1.4 (27.0–31.0)
Stylet conus	11.1 ± 0.5 (10.5–11.5)	10.6 ± 0.5 (10.0–11.0)	17.6 ± 0.7 (16.5–18.5)	13.3 ± 0.8 (12.0–14.0)
D.G.O.	5.3 ± 0.3 (5.0–5.5)	5.3 ± 0.4 (5.0–6.0)	4.2 ± 0.3 (4.0–5.0)	4.3 ± 0.5 (4.0–5.0)
O	23.9 ± 0.8 (22.7–24.4)	25.6 ± 1.9 (22.7–28.6)	11.8 ± 0.9 (11.0–13.9)	14.8 ± 1.6 (12.9–16.7)
Anterior end to centre of median bulb	64 ± 2.5 (61–67)	64 ± 2.6 (60–67)	85 ± 2.1 (82–88)	74 ± 1.8 (72–77)
Anterior end to excretory pore	89 ± 3.6 (84–92)	83 ± 3.9 (77–87)	127 ± 2.5 (124–132)	105 ± 9.5 (97–117)
Pharynx length	108 ± 10.9 (95–117)	118 ± 3.8 (114–123)	156 ± 6.8 (147–168)	128 ± 2.8 (124–131)
Pharyngeal overlap	20.8 ± 2.2 (18.0–23.0)	21.7 ± 2.7 (18.0–26.0)	17.3 ± 2.5 (14.0–20.0)	6.8 ± 3.1 (5.0–13.0)
Max. body diam.	23.9 ± 0.6 (23.0–24.5)	23.8 ± 1.0 (23.0–25.0)	30.8 ± 1.6 (29.0–33.0)	30.7 ± 1.6 (29.0–33.0)
Anal body diam.	17.5 ± 0.4 (17.0–18.0)	14.7 ± 0.8 (14.0–16.0)	21.1 ± 0.7 (20.0–22.5)	20.3 ± 1.3 (18.5–22.0)
Tail	10.6 ± 1.4 (9.0–12.0)	16.3 ± 1.2 (15.0–18.0)	25.4 ± 2.7 (22.5–32.0)	17.8 ± 1.5 (16.0–20.0)
Tail annuli	7.3 ± 1.0 (6–8)	–	16.6 ± 1.9 (14–19)	10.7 ± 0.8 (10–12)
Phasmid to terminus	30.5 ± 2.1 (28.0–33.0)	–	34.5 ± 5.0 (30.0–40.0)	23.8 ± 4.6 (21.0–33.0)
Spicules	–	22.0 ± 0.7 (21.0–23.0)	–	–
Gubernaculum	–	9.6 ± 0.9 (9.0–11.0)	–	–

[a] Abbreviations are defined in Siddiqi (2000).

Stylet robust, 2.8–3.2 times longer than labial region diam. Basal knobs rounded slightly convex anteriorly, 6.0–6.5 μm wide. Dorsal pharyngeal gland opening 4.0–5.0 μm posterior to stylet base. Procorpus of pharynx cylindrical, with slight depression just anterior to median bulb, 36.8 ± 2.1 (34–40) μm long. Median pharyngeal bulb well developed, broadly oval, 13.0–15.0 × 10.5–12.0 μm, occupying 8–10 annuli, valvular apparatus 3.0 μm long, located at 53.9 ± 1.0 (53–56)% of pharyngeal length. Isthmus 26.3 ± 1.0 (25–28) μm long, encircled by nerve ring at mid-point. Pharyngeal glands short, with three nuclei, slightly overlapping intestine dorsally for 2–4 annuli. Nerve ring enveloping isthmus at middle, at 85 ± 2.9 (81–89) μm from anterior end. Excretory pore usually located near middle of isthmus level. Hemizonid distinct, located at anterior to excretory pore, extending for *ca* 1.0–1.5 body annuli width, just anterior to excretory pore. Reproductive system with both genital branches equally developed; anterior branch 158 ± 13.0 (144–182) μm long, posterior branch 143 ± 14.9 (122–160) μm long. Vulva clearly posterior to mid-body, without a distinct epiptygma. Vagina with internal walls slightly sclerotised, 11.8 (11.0–12.5) μm long. Ovaries with a single row of oocytes. Phasmids pore-like, 5.0 ± 1.1 (4–6) annuli anterior to level of anus or 5.4 ± 2.2 (3.0–9.0) μm anterior to anus. Tail short, of variable shape, conoid-rounded, terminus striated and cuticle at tail tip 2.6 ± 0.2 (2.5–3.0) μm wide.

3.2.5. *Rotylenchus robustus (de Man, 1876) Filipjev, 1936*

Fig. 8 and Table 6.

Female: Body large, habitus usually forming a spiral. Lateral fields with four smooth equidistant lines, 11.1 ± 0.8 (10.0–12.0) μm wide at mid-body, approximately one-fourth as wide as body diam. Regular areolation of lateral fields (external bands) observed in pharyngeal region, an irregularly areolated along-body (Fig. 8). Cuticle 1.5–2.0 μm thick, clearly annulated, annuli 1.5–2.0 μm wide at mid-body. Labial region hemispherical, set off from body by a constriction, bearing 6–8 annuli, irregularly divide longitudinally,

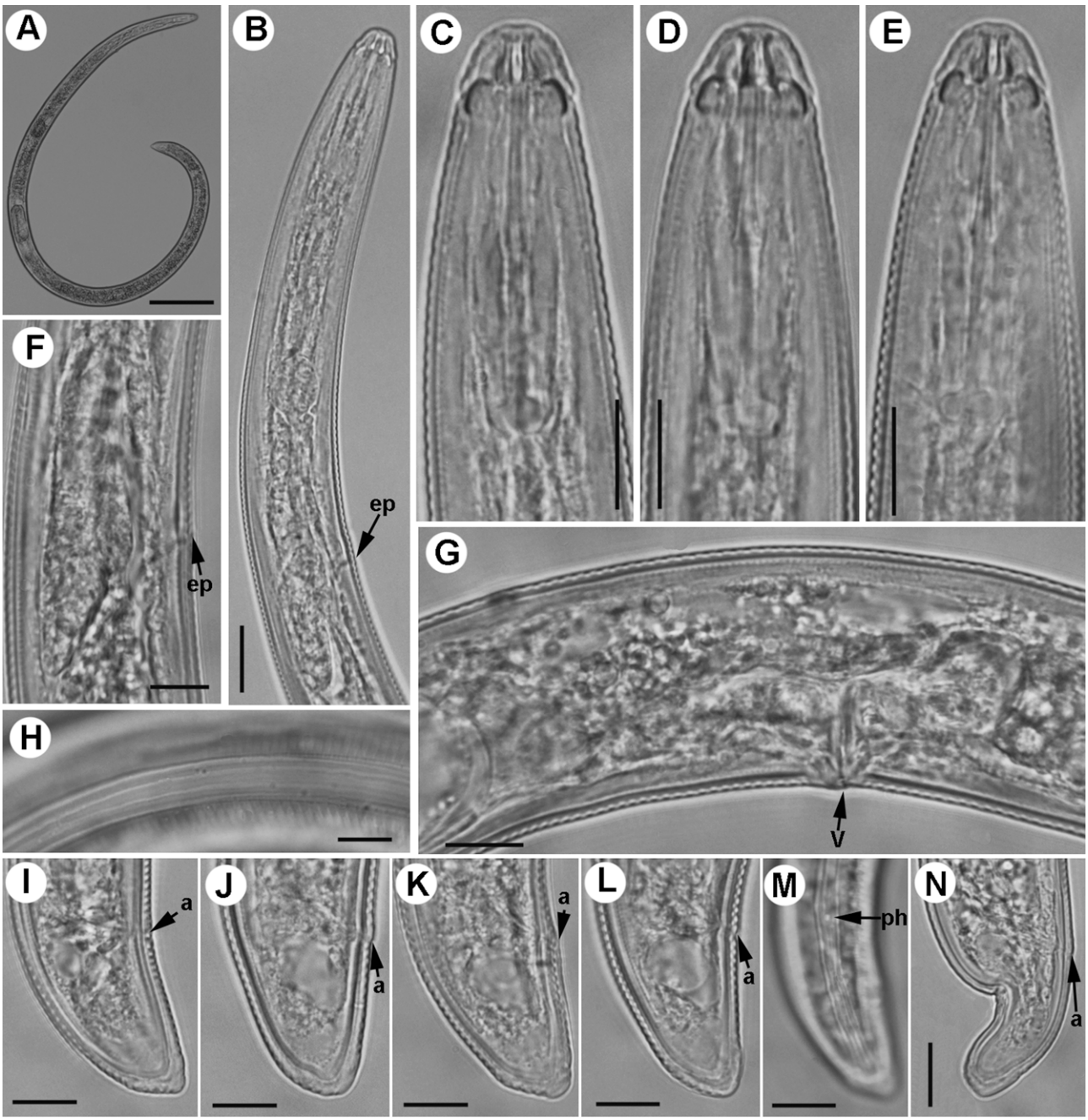

Fig. 6. Light micrographs of *Rotylenchus buxophilus* Golden, 1956 (A) Female habitus. (B) Female anterior body region. (C–E) Female lip regions. (F) Detail of pharyngeal region. (G) Vulval region. (H) Lateral fields at mid-body. (I–M) Female tail regions. (N) Abnormal female tail. *Abbreviations*: a: anus; ep: excretory; ph: phasmid (scale bars: A: 100 μm; B: 20 μm; C–N: 10 μm).

particularly the 2–3 basal annuli. Labial disc distinct under SEM, rounded. Centrally located on the oral disc is the oval opening of the prestoma without any labial sensillae surrounding (Fig. 8). The oral disc is clearly separated from the first annulus of the lip region, which is divided into six sectors, with lateral sectors, bordering the amphidial apertures, smaller than the subventral and subdorsal sectors. Each amphidial opening appears as a half ellipse, *i.e.* a wide slit with a curved distal margin between the oral disc and the lateral sectors of the first lip annulus. Labial framework well developed, 4.7 ± 0.4 μm (4–5) long, posterior margin at level of 6th or 8th body annulus. Stylet robust, 3.6–4.1 times longer than labial region diam. Basal knobs rounded, 7.5–9.0 μm wide, at level of 22–26th annulus posterior to labial region. Pharyngeal glands sacciform, with three nuclei, overlapping intestine dorsally for 22–46 annuli. Excretory pore usually located near pharyngo-intestinal junction level. Reproductive system with both genital branches equally developed. Vulva slightly posterior to mid-body, with a distinct epiptygma. Ovaries with a single row of oocytes, spermathecae rounded, with sperm (1.5–2.0 μm wide). Phasmids pore-like, 2.8 ± 1.1 (1–4) annuli anterior to level of anus or 4.5 ± 1.8 (3.0–8.0) μm anterior to anus. Tail short, hemispherical, with 10–21 annuli, terminus striated and cuticle at tail tip 6.8 ± 0.4 (6.0–7.0) μm wide.

Male: Common, habitus an open C shape. Lip region more distinctly set off and more elevated than in female. Testis single, outstretched. Bursa crenate 76.2 ± 4.8 (68.0–82.0) μm long,

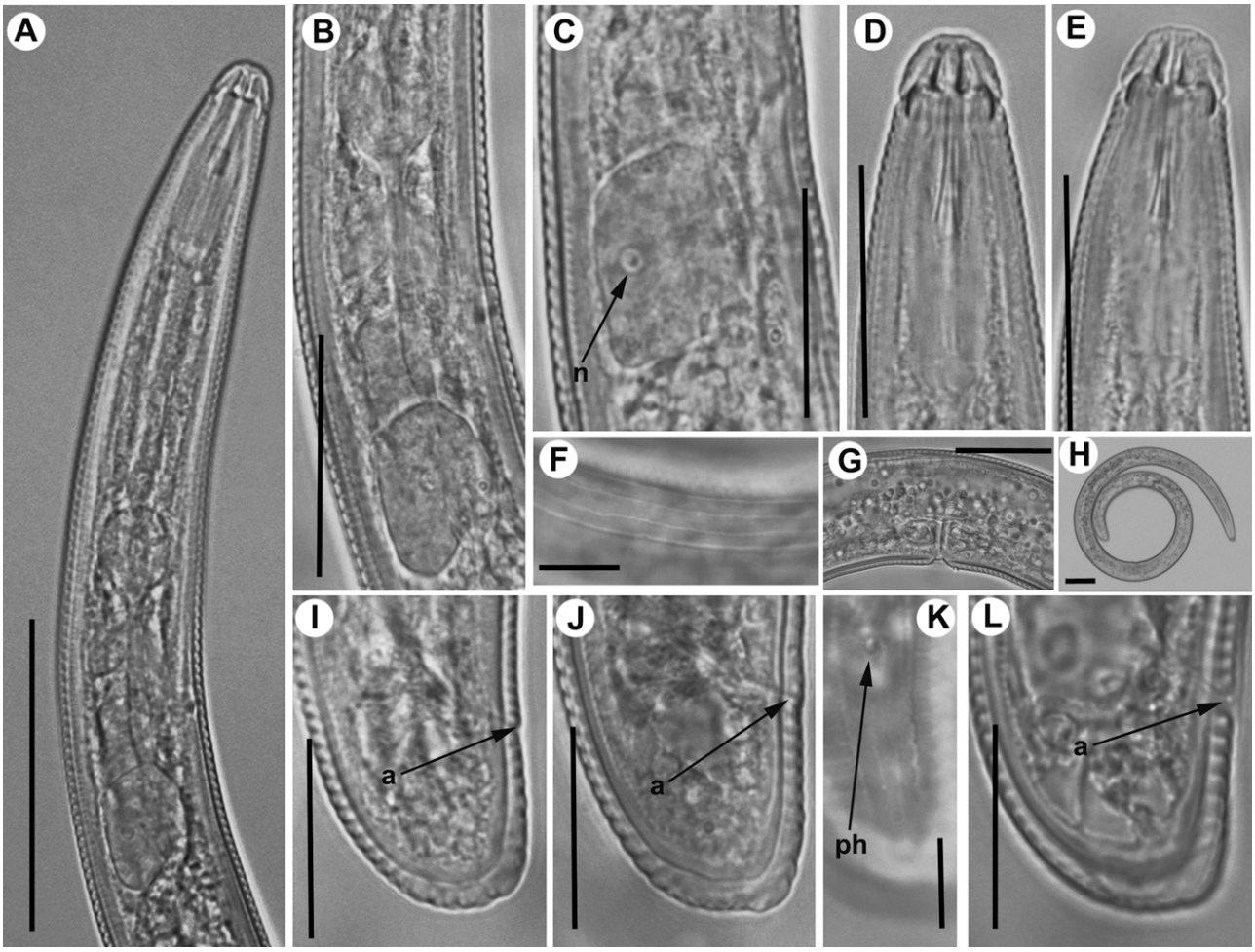

Fig. 7. Light micrographs of *Rotylenchus pumilus* (Perry et al., 1959) Sher, 1961. (A) Female pharyngeal regions. (B, C) Details of pharyngeal gland. (D, E) Female anterior body region. (F) Detail of lateral fields at mid-body. (G) Vulval region. (H) Female habitus. (I, J, L) Female tail regions. (K) Detail of phasmid. *Abbreviations*: a: anus; n: gland nucleus; ph: phasmid (scale bars: A, H: 50 μm; B–E, G: 25 μm; F, K: 10 μm; I, J, L: 20 μm).

completely surrounding tail which is tapering with a rounded-pointed tip. Spicules ventrally arcuate. Gubernaculum protrusible, with prominent titillae distally.

3.3. Molecular characterisation and phylogenetic position of *Rotylenchus paravitis* n. sp. within the genus and other Hoplolaimidae

Similarity values from D2-D3 expansion segments of 28S and ITS1-rRNA among species of *Rotylenchus* are presented in Table 7. Interspecific variations for the D2-D3 sequence among *Rotylenchus* species retrieved from GenBank and *R. paravitis* n. sp. varied from 34 to 57 nucleotides (5–12%). Phylogenetic analysis (BI and ML) of Rotylenchoidinae and Hoplolaiminae based on D2-D3 expansion segments of 28S-rRNA of a multiple alignment including 82 sequences of 574 bp in length showed 4 moderately or highly supported lineages in the genus *Rotylenchus* (Fig. 9): (i) *R. incultus*, *R. goodeyi*, *R. laurentinus*, *R. buxophilus* and *R. pumilus*; (ii) *R. montanus*, *Rotylenchus* sp. SAS-2006, and *R. brevicaudatus*; (iii) *R. robustus*, *R. uniformis*, *R. magnus* and *R. jaeni*, *R. cazorlaensis*; and (iv) *R. eximius*, *R. vitis* and *R. paravitis* n. sp. (Fig. 9). *Helicotylenchus* species formed three highly supported clades, *Scutellonema* formed a single highly supported clade, and *Hoplolaimus* and *Aorolaimus* clustered together in a separate clade together with *R. unisexus* (Fig. 9). *Rotylenchus paravitis* n. sp. formed a poorly supported clade with *R. eximius and R. vitis*, but occupied a monophyletic position among the other genera of Hoplolaimidae (*Helicotylenchus*, *Hoplolaimus* and *Scutellonema*) included in the analysis (Fig. 9).

D2-D3 expansion segments of 28S-rRNA did not refute the monophyly of the genera *Rotylenchus* ($P = 0.071$), *Helicotylenchus* ($P = 0.572$), *Hoplolaimus* ($P = 1.00$), even regarding the tree topology in several clades within some of the genera (Table 8). The exclusion of some species strongly associated to *Helicotylenchus* (*viz. R. conicaudatus*, HQ700698) and other not so strongly associated to *Hoplolaimus* and *Aorolaimus* (*R. unisexus*, EU280799) did not refute the monophyly of *Rotylenchus* ($P = 0.635$) (Table 8). Similar results were obtained for the analysis based on the partial 18S. However, the absence of some sequences in genus *Hoplolaimus* or some *Rotylenchus* species (*viz. R. conicaudatus* and *R. unisexus*), may be the cause of these results. In both cases the constriction of the genera *Rotylenchus*, *Helicotylenchus*, *Hoplolaimus* and *Scutellonema* did not refute to the monophyly of these genera ($P = 0.064$ for D2-D3 and $P = 0.298$ for partial 18S).

ITS1-rRNA from *R. paravitis* n. sp. sequence differed to the aligned sequences of *Rotylenchus* species in a range from 84 to 155 nucleotides (18–34%). Since only seven partial 18S-rRNA sequences from *Rotylenchus* species are deposited in GenBank, phylogenetic analysis with this gene was carried out including 18S sequences from six *Helicotylenchus* species. The alignment for 28 ITS1-rRNA sequences of *Rotylenchus* samples was 800 bp long. After discarding ambiguously aligned regions from the alignment, the ITS1 dataset included 448 bp. The 50% majority rule consensus phylogenetic tree

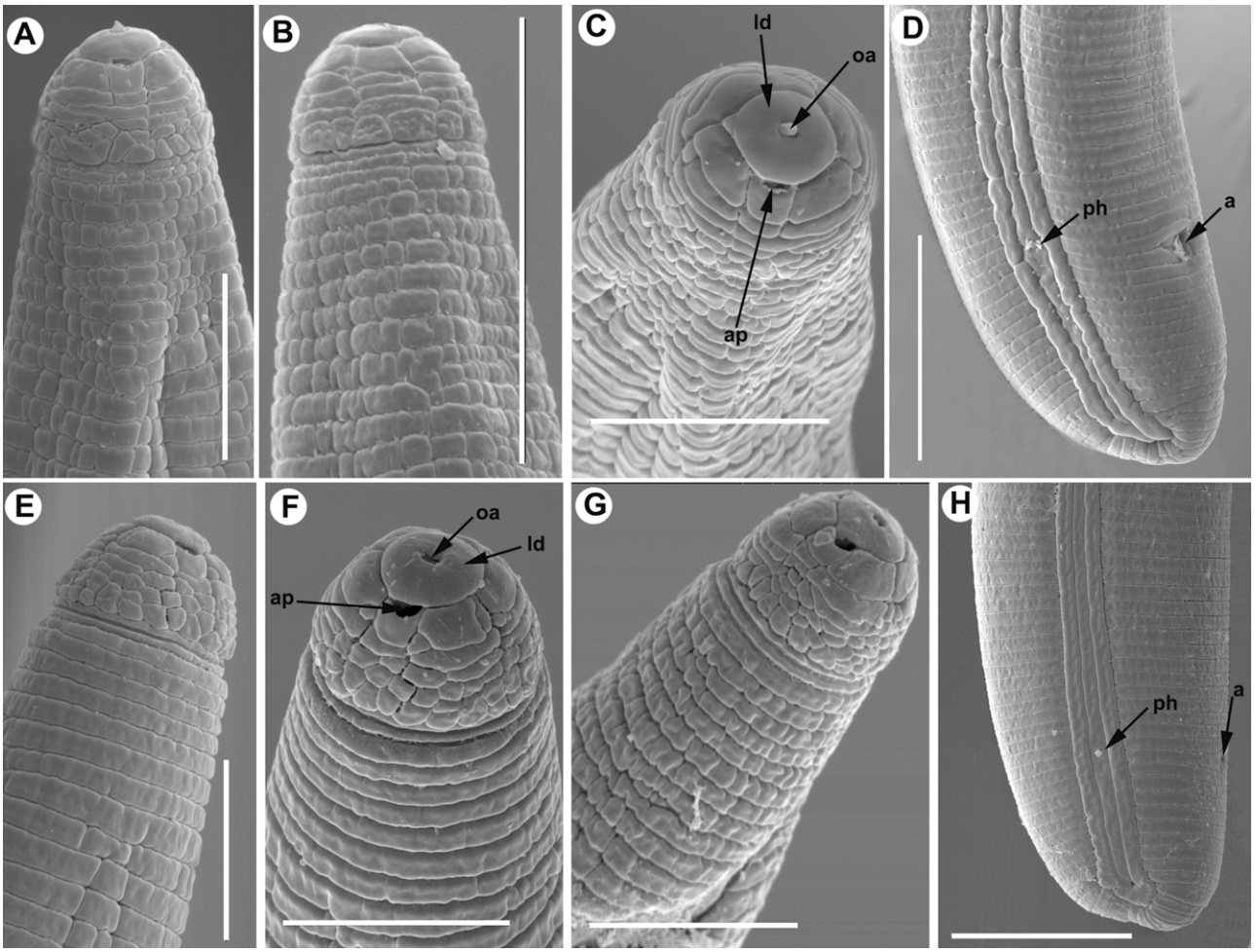

Fig. 8. Scanning electron microscope photographs of *Rotylenchus robustus* (de Man, 1876) Filipjev, 1936 from Lucena del Puerto, Huelva province, southern Spain (A–D) and Tomales, California, USA (E–H). (A, B, E) Female lip region, lateral views, showing basal lip annulus with longitudinal striations. (C, F, G) En face view showing oral aperture (oa), amphid (ap) and labial disc (ld). (D, H) Female tail region showing anus (a) and phasmid (ph) (scale bars: A, C, E–G: 10 μm; B, D, H: 10 μm).

generated from the ITS1-rRNA alignment by BI analysis under the TVM + G model is presented in Fig. 10. The tree topologies between ML and BI were congruent and showed a similar clustering topology to that obtained for D2-D3, including 3 clades with similar species in each one. *Rotylenchus paravitis* n. sp. which does not form supported clades with any of the other *Rotylenchus* species (Fig. 10). On the other hand, *R. robustus* formed a well supported clade with *R. magnus* and *R. jaeni*. *Rotylenchus vitis* formed a moderately supported clade with *R. iranicus*, but not with the most similar species *R. paravitis* n. sp., which occupied a basal position in a clade with *R. jaeni*, *R. magnus*, *R. robustus*, *R. cazorlaensis* and *R. eximius* (Fig. 10). Similarly, the alignment for partial 18S-rRNA of 8 *Rotylenchus* samples and other Rotylenchoidinae and Hoplolaiminae in the GenBank with 1713 positions in length showed a highly supported clade with *R. uniformis*, *R. robustus*, and *R. jaeni*, a moderately supported clade formed by *R. paravitis* n. sp. and *R. vitis*, whereas *R. goodeyi*, *R. eximius*, and *Rotylenchus* sp. JH-2004 were clearly separated from the former, and *Helicotylenchus* species formed two well supported clades (Fig. 11). Similarity values from the partial 18S-rRNA sequence of *R. paravitis* n. sp. with those deposited in GenBank were high and ranged from 95% for *Rotylenchus* sp. (AY284608) to 98% for *R. vitis* (JN032583). Similarly, the alignment for partial 18S-rRNA of 8 *Rotylenchus* samples and others Rotylenchoidinae and Hoplolaiminae in the GenBank with 1713 positions in length showed a highly supported clade with *R. uniformis*, *R. robustus*, and *R. jaeni*, a moderately supported clade formed by *R. paravitis* n. sp. and *R. vitis*, whereas *R. goodeyi*, *R. eximius*, and *Rotylenchus* sp. JH-2004 were clearly separated from the former, and *Helicotylenchus* species formed two well supported clades (Fig. 11).

There was not any sequence of *COI* from *Rotylenchus* species deposited in GenBank, so only the partial *COI* sequences of this study have been used. Similarity values of *COI* sequences of *R. paravitis* n. sp. with those of other *Rotylenchus* species ranged from 90% for *R. eximius* (JX015401, JX015402), 87% for *R. vitis* (JX015417, JX015418), 82% for *R. cazorlaensis* (JX015399, JX015400), 77% for *R. robustus* (JX015411–JX015414), to 76% for *R. magnus* (JX015408–JX015410). There was no intraspecific variation among *COI* of different populations from the same species, except for *COI* for *R. robustus* which showed 92% similarity (321/359 bp) between the two Spanish isolates and 84% similarity (298/354 bp) with USA isolate. The *COI* alignment consisted of 22 sequences with 409 bp in length. The 50% majority rule consensus phylogenetic tree generated from the *COI* alignment by BI analysis under the GTR + I + G model is presented in Fig. 11. The tree topologies between ML and BI were congruent. The *COI* tree showed the same clade that appears in D2-D3 or ITS1 trees, separating *R. paravitis* n. sp. from *R. vitis* and *R. eximius*, and a major clade including *R. cazorlaensis*, *R. buxophilus*, *R. incultus*, *R. laurentinus*, *R. jaeni*, *R. magnus*, and a moderately supported sub-clade with *R. robustus* clearly separated by its geographical origin (Spanish or American isolates) (Fig. 12).

Table 6
Morphometrics of *Rotylenchus robustus* (de Man, 1876) Filipjev, 1936 from Tomales (California, USA) and from Lucena del Puerto (Huelva province, southern Spain). All measurements are in μm and in the form: mean ± s.d. (range).[a]

Character	*R. robustus* – population			
	Tomales, California, USA		Lucena del Puerto, Spain	
	Females	Males	Females	Males
n	12	9	9	6
L	1429 ± 83.6 (1207–1533)	1311 ± 129.7 (1117–1555)	1423 ± 143.4 (1178–1583)	1203 ± 57.3 (1117–1272)
a	33.0 ± 2.7 (29.4–37.6)	37.3 ± 2.4 (33.5–40.3)	34.6 ± 2.8 (30.2–37.4)	38.8 ± 1.0 (37.2–39.8)
b	12.9 ± 0.9 (11.4–14.3)	12.6 ± 0.7 (11.6–14.1)	13.5 ± 1.2 (11.2–14.9)	13.7 ± 0.6 (13.1–14.6)
b′	7.1 ± 0.7 (6.3–8.3)	6.7 ± 0.5 (6.2–7.5)	7.2 ± 0.8 (5.8–8.5)	6.8 ± 0.3 (6.5–7.2)
c	54.6 ± 5.6 (42.7–63.8)	39.3 ± 4.0 (34.3–45.7)	65.2 ± 8.3 (57.8–80.4)	40.2 ± 3.2 (36.0–45.4)
c′	0.8 ± 0.1 (0.7–0.9)	1.3 ± 0.1 (1.2–1.5)	0.7 ± 0.05 (0.6–0.8)	1.4 ± 0.1 (1.2–1.5)
V or *T*	54.0 ± 1.2 (53.0–57.0)	39.8 ± 8.4 (28.9–51.6)	53.8 ± 0.7 (53.0–55.0)	41.6 ± 8.0 (30.6–51.7)
G_1	18.3 ± 3.7 (14.0–23.9)	–	17.1 ± 3.0 (13.2–21.6)	–
G_2	18.0 ± 4.3 (12.0–23.6)	–	16.3 ± 2.9 (12.0–21.1)	–
Stylet	46.8 ± 2.1 (43.0–50.0)	41.7 ± 1.7 (40.0–45.0)	49.6 ± 1.7 (46.0–51.0)	43.5 ± 2.1 (41.0–47.0)
Stylet conus	23.2 ± 1.6 (21.0–26.0)	21.4 ± 0.7 (20.5–22.5)	25.3 ± 0.8 (24.0–26.5)	21.8 ± 0.9 (21.0–23.0)
D.G.O.	7.4 ± 0.9 (6.5–9.0)	7.1 ± 0.8 (6.0–9.0)	6.7 ± 0.4 (6.0–7.0)	5.3 ± 0.4 (5.0–6.0)
O	15.8 ± 1.8 (13.3–19.6)	16.9 ± 1.9 (14.4–20.9)	13.5 ± 0.7 (12.0–14.6)	12.2 ± 0.4 (11.6–12.8)
Anterior end to centre of median bulb	113 ± 7.9 (100–126)	104 ± 6.3 (91–110)	105 ± 3.3 (99–109)	88 ± 4.7 (82–95)
Anterior end to excretory pore	150 ± 15.7 (134–176)	162 ± 13.7 (135–178)	162 ± 13.8 (143–179)	138 ± 4.5 (131–143)
Pharynx length	203 ± 19.4 (178–234)	194 ± 12.1 (181–213)	198 ± 10.5 (181–210)	177 ± 11.0 (165–195)
Pharyngeal overlap	47.9 ± 9.0 (39.0–67.0)	50.2 ± 3.6 (45.0–55.0)	46.1 ± 4.2 (41.0–52.0)	44.2 ± 3.4 (41.0–49.0)
Max. body diam.	43.5 ± 3.6 (38.0–49.0)	35.2 ± 3.4 (31.0–41.0)	41.1 ± 1.3 (39.0–43.0)	31.0 ± 1.1 (30.0–32.0)
Anal body diam.	34.1 ± 2.4 (30.0–37.0)	25.1 ± 3.7 (19.0–30.0)	31.4 ± 2.2 (29.0–36.0)	21.6 ± 1.1 (20.5–23.5)
Tail	26.4 ± 2.4 (23.0–32.0)	33.5 ± 3.3 (26.5–38.0)	22.0 ± 2.7 (19.0–26.0)	30.0 ± 1.7 (28.0–32.0)
Tail annuli	14.3 ± 2.2 (13–21)	–	14.0 ± 2.2 (10–17)	–
Phasmid to terminus	34.2 ± 4.1 (28.0–43.0)	–	26.6 ± 2.2 (22.0–30.0)	–
Spicules	–	37.1 ± 2.8 (33.0–41.0)	–	35.7 ± 2.0 (33.0–38.0)
Gubernaculum	–	18.6 ± 1.6 (16.0–21.0)	–	17.7 ± 1.0 (16.0–19.0)

[a] Abbreviations are defined in Siddiqi (2000).

The alignment generated from *hsp90* sequences from *R. paravitis* n. sp. and *R. vitis* showed the presence of insertions in the *hsp90* sequence of *R. paravitis* n. sp. After discarding ambiguously aligned regions from the alignment, the size was 150 bp with a similarity of 81% (122/150 and 5 gaps, 3%) between them. Finally, the *hsp90* alignment consisted of 35 sequences with 244 bp in length. The 50% majority rule consensus phylogenetic tree generated from the *hsp90* alignment by BI analysis under the K80 + G model is presented in Fig. 13. The *hsp90* tree showed that *Rotylenchus* spp. clustered together with *H. pseudorobustus*, and *R. paravitis* n. sp. was clearly separated from *R. vitis* and other *Rotylenchus* spp. (Fig. 13).

3.4. Molecular diagnostics of some Rotylenchus species

PCR-D2-D3-28S-RFLP profile for *R. paravitis* n. sp. is given in Fig. 14. The following restriction profiles are obtained for this species: unrestricted PCR – 792 bp; *Ava*I – 395, 267, 130 bp, *Rsa*I – 328, 259, 161, 38, 6 bp; *Bse*NI – 684, 108 bp; *Mva*I – 560, 232 bp; *Hpa*II –215, 206, 164, 145, 62 bp.

Results of PCR with species specific primers are given in Fig. 15. The combinations of the universal TW81 primer with the species specific *R. paravitis*, *R. vitis* or *R. robustus* primers yielded amplicons of approximately 131, 258, or 438 bp in lengths for corresponding species, respectively. No additional bands were observed in any tested samples.

4. Discussion

4.1. Multivariate analysis of morphological characters

Results of multivariate analyses identified size, lip annuli, stylet knobs, cuticle at tail tip, and position of phasmid, the stylet conus

Table 7
Similarity values (%) of rRNA sequences among *Rotylenchus* species. Above diagonal D2-D3 expansion segments of 28S rRNA and below diagonal ITS1 region.[a]

	Rotylenchus spp.																					
Rotylenchus spp.	**01**	02	03	**04**	05	**06**	07	08	09	10	11	12	13	14	15	16	**17**	**18**	19	20	21	22
01. *R. paravitis* n. sp.*		92	-	89	88	92	92	91	93	90	90	89	93	90	93	90	90	93	92	90	94	90
02. *R. agnetis*	-		-	88	89	92	91	88	90	90	90	90	92	90	92	92	90	92	92	89	90	91
03. *R. brevicaudatus*	74	-		-	-	-	-	-	-	-	-	-	-	-	-	-	-	-	-	-	-	-
04. *R. brevicaudatus*	74	-	99		86	89	88	88	87	93	93	86	89	93	88	88	95	89	88	87	88	89
05. *R. buxophilus*	-	-	-	-		97	90	87	87	93	93	86	89	93	89	89	95	89	89	88	87	88
06. *R. buxophilus*	81	-	-	81	-		93	91	91	96	96	90	92	97	92	91	98	92	92	91	91	91
07. *R. cazorlaensis*	77	-	74	74	-	61		90	91	91	92	89	95	92	95	90	91	94	94	91	90	90
08. *R. conicaudatus*	62	-	62	62	-	69	59		90	87	88	88	90	88	90	88	90	91	91	89	89	88
09. *R. eximius*	74	-	71	70	-	60	73	56		89	89	89	92	89	92	89	89	92	92	90	92	90
10. *R. goodeyi*	-	-	-	-	-	-	-	-	-		99	88	90	99	90	89	95	90	90	89	88	89
11. *R. incultus*	66	-	65	65	-	83	66	66	61	-		88	90	99	90	90	95	90	90	90	88	89
12. *R. iranicus*	67	-	67	67	-	71	65	67	63	-	68		89	88	90	88	88	90	90	87	87	88
13. *R. jaeni*	77	-	64	73	-	63	81	59	71	-	72	68		90	98	90	90	96	96	90	92	90
14. *R. laurentinus*	65	-	65	65	-	83	65	66	61	-	68	72	68		90	90	95	90	90	90	89	89
15. *R. magnus*	77	-	75	74	-	63	85	59	73	-	65	68	92	67		90	90	97	97	90	92	90
16. *R. montanus*	65	-	65	64	-	64	65	61	62	-	67	65	65	66	65		90	91	90	88	89	99
17. *R. pumilus*	81	-	-	81	-	97	62	68	59	-	83	71	62	83	62	64		91	90	89	90	90
18. *R. robustus*	73	-	70	69	-	59	80	59	70	-		67	81	65	85	65	58		99	91	92	90
19. *R. uniformis*	-	-	-	-	-	-	-	-	-	-	-	-	-	-	-	-	-	-		90	92	90
20. *R. unisexus*	69	-	64	64	-	68	66	65	65	-	72	72	66	67	66	65	-	62	-		89	88
21. *R. vitis*	72	-	62	61	-	68	65	62	63	-	64	64	66	63	67	72	68	66	-	65		89
22. *Rotylenchus* sp.	66	-	65	64	-	87	65	61	63	-	65	65	65	66	65	98	86	81	-	66	72	

Accessions numbers (D2-D3, ITS1, respectively): **1**: **JX015422**, **JX015434**; 2: EU280795; 3: DQ309587; **4**: **JX015419**, **JX015430**; 5: FJ485647; **6**: **JX015421**, **JX015432**; 7: EU280792, EU373671; 8: HQ700698; HQ700700; 9: EU280794, EU373664; 10: DQ328756; 11: EU280797; EU373673; 12: HQ700697; HQ700699; 13: EU280791, EU373662; 14: EU280798, EU373667; 15: EU280789, EU373665; 16: DQ328743, EU280800; **17**: **JX015423**, **JX015435**; **18**: **JX015424**, **JX015437**; 19: DQ328737; 20: EU280799; EU373675; 21: JN032581, JN032582; 22: DQ328742, EU280802.

[a] Newly obtained sequences are in bold letters. (–) Not available.

and orifice of dorsal gland as key characters to differentiate *R. vitis* and *R. paravitis* n. sp. from those of *R. robustus*. However, no characters could be found to clearly discriminate between specimens of *R. vitis* and *R. paravitis* n. sp. since their values overlapped for the two species. Moreover, their degree of variation was comparable to that observed among specimens belonging to each of the two populations of *R. robustus*. Consequently, on the basis of this morphometric multivariate analysis as well as morphological cryptic species, since both taxa are cryptic to human perception largely due to the lack of conspicuous differences in morphometric appearance (Palomares-Rius et al., 2010).

4.2. Comparative morphology and morphometry of Rotylenchus paravitis n. sp. and other Rotylenchus spp. studied

Delimiting closely related nematode species is a particularly difficult issue. For this reason, Castillo and Vovlas (2005) established a specific matrix code for *Rotylenchus* spp. according to the following: Group A: 1 = lip region (l.r.) annulation absent or smooth; 2 = l.r. with 2–3 annuli; 3 = l.r. with 4 annuli; 4 = l.r. with 5 annuli; 5 = l.r. with 6 annuli; 6 = l.r. with 7–8 annuli; 7 = l.r. with 9–10 annuli. Group B: 1 = l.r. hemispherical; 2 = l.r. rounded; 3 = l.r. conoid; 4 = l.r. truncate. Group C: 1 = only in pharyngeal region (ph. reg.); 2 = in ph. reg. and irregularly at mid-body; 3 = in ph. reg. and incompletely at mid-body; 4 = in ph. reg. and near phasmids; 5 = whole body length except tail region; 6 = whole body length included tail region; 7 = incompletely along whole body. Group D: 1 = punctuated along body annuli; 2 = longitudinally striated in ph. reg.; 3 = longitudinally striated over whole body; 4 = without body striations. Group E: 1 = <30 μm; 2 = by 30–35.9 μm; 3 = by 36–40.9 μm; 4 = >41 μm. Group F: 1 = <2 μm; 2 = by 2–6.9 μm; 3 = by 7–12 μm; 4 = >12 μm. Group G: 1 = <5 μm; 2 = by 6–20.9 μm; 3 = by 21–30.9 μm; 4 = by 31–40.9 μm; 5 = >41 μm. Group H: 1 = hemispherical; 2 = rounded; 3 = conoid; 4 = pointed; 5 = with ventral projection. Group I: 1 = <50%; 2 = by 50 to 70%; 3 = >70%. Group J: 1 = present; 2 = absent. Group K: 1 = >5 annuli anterior to anus; 2 = from 5 anterior to 5 posterior to anus; 3 = >5 annuli posterior to anus. *Rotylenchus paravitis* sp. n. is very close to *R. vitis* in general morphology and morphometry, since most of the morphometric characters are within the same range, including de Man ratios, D.G.O., *O*, spicules and gubernaculum. Morphologically *R. paravitis* n. sp. can be also distinguished from the most similar species by a number of particular characteristics resulting from its specific matrix code

Table 8
Results of the SH-tests for alternative hypotheses using ML trees.

Topologies and hypothesis tested	D2-D3			18S		
	$-Ln\,L$	Difference of $-Ln\,L$	P^*	$-Ln\,L$	Difference of $-Ln\,L$	P^*
ML tree	6727.44	Best		5810.80	Best	
All *Rotylenchus* spp. constrained into one group	6752.96	25.52	0.071	5814.55	3.75	0.298
All *Helicotylenchus* spp. constrained into one group	6733.37	5.93	0.572	5810.80	0.00	1.00
All *Hoplolaimus* spp. constrained into one group[a]	6727.44	0.00	1.00	Non-available	–	–
Grouping separately *Rotylenchus–Helicotylenchus–Hoplolaimus–Scutellonema*[a]	6753.99	26.55	0.064	5814.55	3.75	0.298
All *Rotylenchus* spp. constrained, with exception of *R. conicaudatus* + *R. unisexus*	6729.92	2.48	0.635	Non-available	–	–

[*] $P < 0.05$ indicates the significant differences between the two inferred tree topology.

[a] Non available partial 18S sequences for *Hoplolaimus* or some specific *Rotylenchus* sequences in GenBank.

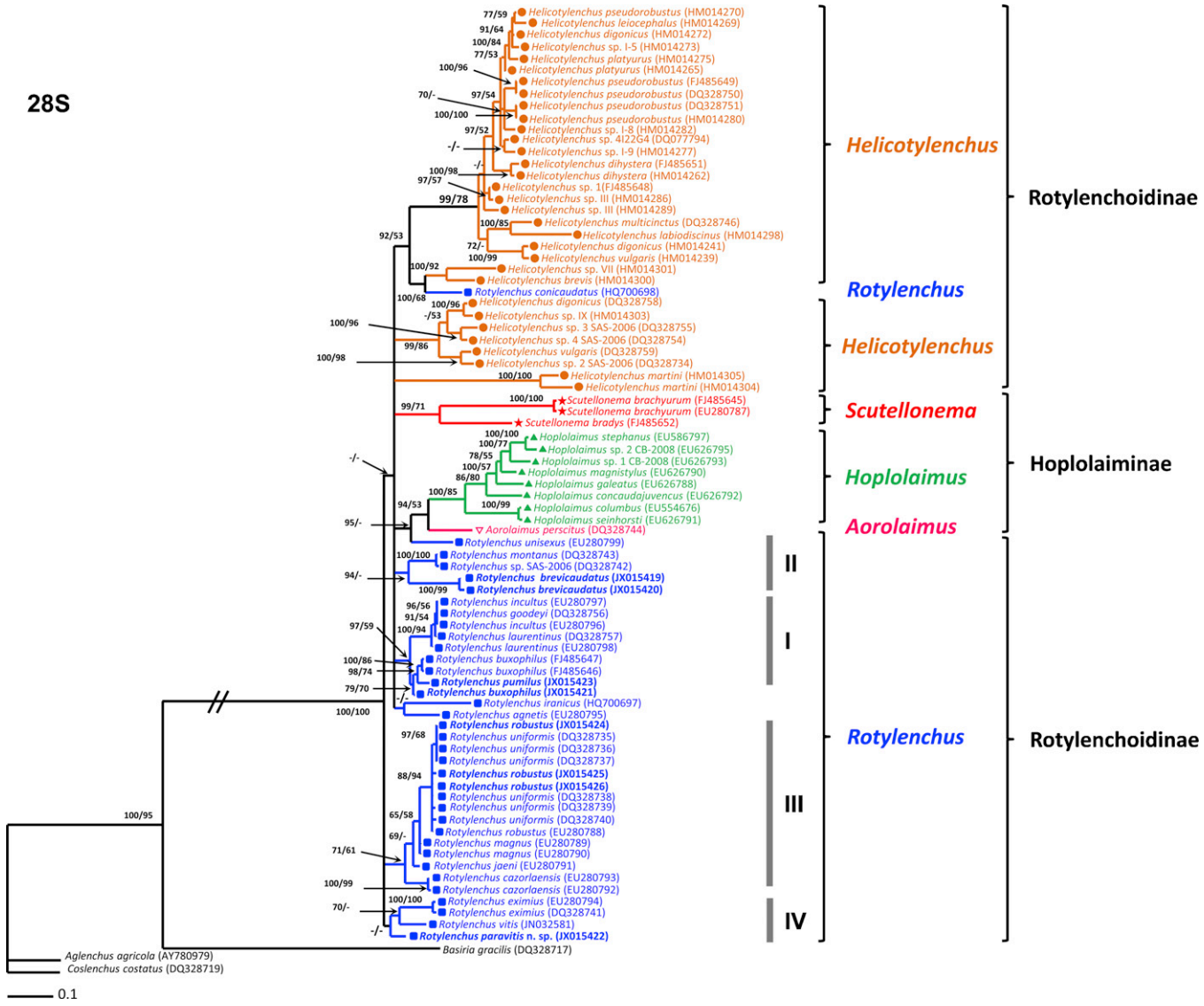

Fig. 9. The 50% majority rule consensus tree from Bayesian analysis generated from the D2-D3 of 28S-rRNA gene dataset with the TVM + I + G model. Posterior probabilities more than 65% are given for appropriate clades; bootstrap values greater than 50% are given on appropriate clades in ML analysis. Newly obtained sequences are in bold letters.

(A6,7, B4, C1, D4, E4, F2, G5, H1,2, I1,2, J1, K1 *sensu* Castillo and Vovlas, 2005). It is also close to *R. cazorlaensis*, *Rotylenchus capitatus* Eroshenko, 1981, *Rotylenchus elegans* (Khan and Khan, 1982) Fortuner, 1987, *Rotylenchus fabalus* Baydulova, 1984, *R. iranicus* Atighi, Pourjam, Pedram, Cantalapiedra-Navarrete, Palomares-Rius and Castillo, 2011, *R. labiodiscus* Wouts and Sturhan, 1999, *R. montanus* Vovlas, Subbotin, Troccoli, Liébanas and Castillo, 2008, and *R. troncapitatus* Scotto La Massèse and Germani, 1998. It differs from *R. cazorlaensis* by lip annuli (7–9 narrow annuli not divided longitudinally *vs.* 6–7 annuli, irregularly divided into blocks), first lip annulus (undivided *vs.* divided into six sectors), distance of orifice of dorsal pharyngeal gland to stylet base (4–7 *vs.* 8.5–11.5 μm), stylet length (44–50 *vs.* 46.5–56.5 μm), phasmid position (12–24 annuli anterior to level of anus *vs.* 0–4 annuli posterior to anus); spicule length (33 *vs.* 42–48 μm), and gubernaculum length (13 *vs.* 19.5–25 μm). It differs from *R. capitatus* by body and stylet length (1383–1856, 44–50 *vs.* 680–850, 26–29 μm, respectively), lip region shape (truncate lip region with 7–9 annuli, continuous with body contour *vs.* truncate with 7–8 annuli, slightly set off from body), and female tail shape (hemispherical *vs.* conoid). It differs from *R. elegans* by body and stylet length (1383–1856, 44–50 *vs.* 500–600, 22–25 μm, respectively), and position of phasmids (12–24 annuli anterior to level of anus *vs.* at 5–8 annuli anterior to anus). It differs from *R. fabalus* by lip region shape (truncate lip region with 7–9 annuli, continuous with body contour *vs.* conoid, without annulation, continuous with body contour), tail tip (regularly annulated *vs.* smooth), phasmid position (12–24 annuli anterior to level of anus *vs.* 0–2 annuli anterior to anus), and presence *vs.* absence of males. It differs from *R. iranicus* by body length (1383–1856 *vs.* 954–1237 μm), lip region shape (truncate lip region with 7–9 annuli, continuous with body contour *vs.* hemispherical, with 5–6, rarely 7 annuli and set off from body), pharyngeal glands overlapping (53–57 *vs.* 3–16 μm long), female tail shape (hemispherical with regularly annulated tip *vs.* short, rounded, slightly conoid in some specimens, and typical smooth end). It differs from *R. labiodiscus* by body and stylet length (1383–1856, 44–50 *vs.* 820–980, 33–37 μm, respectively), and position of phasmids (12–24 annuli anterior to level of anus *vs.* located from five annuli anterior to one annulus posterior to anus level). It differs from *R. montanus* by lip region shape (truncate lip region with 7–9 annuli, continuous with body contour *vs.* hemispherical with 6–7 annuli), body and stylet length (1383–1856, 44–50 *vs.* 913–1135,

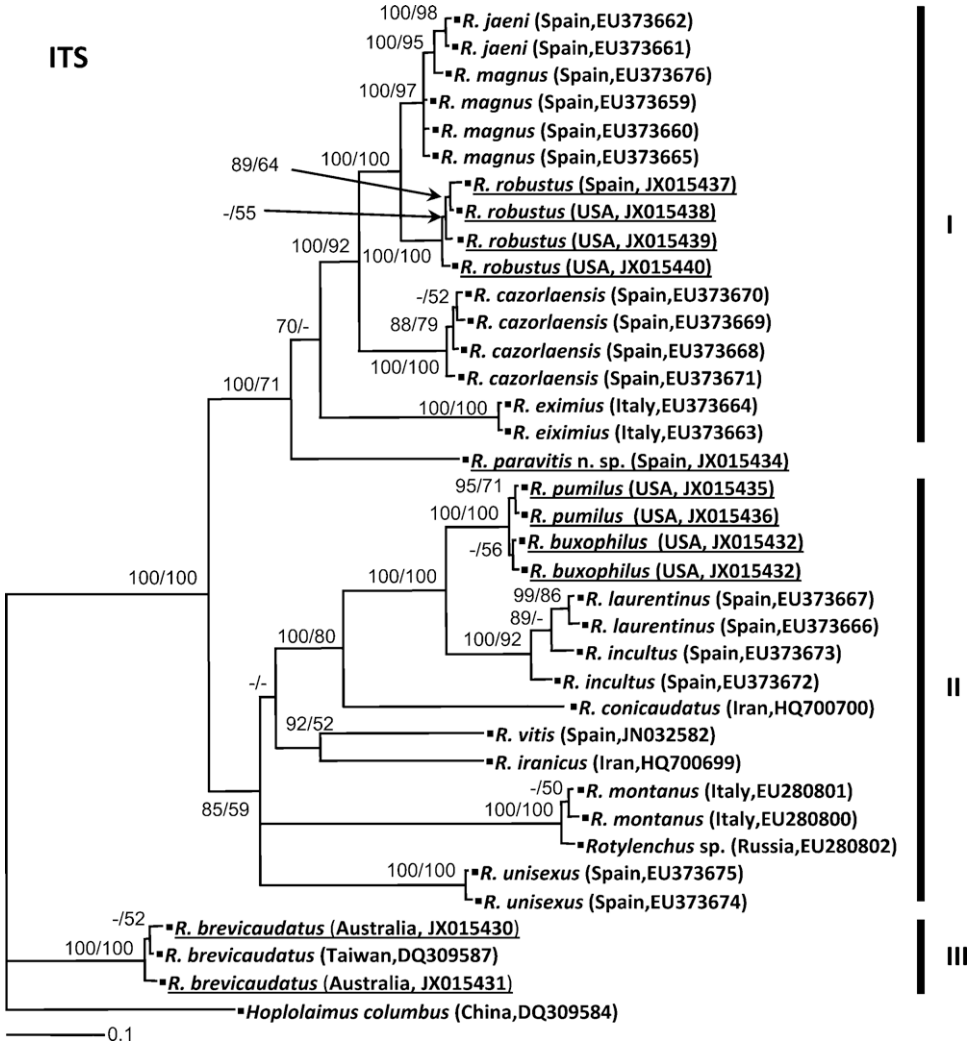

Fig. 10. The 50% majority rule consensus tree from Bayesian analysis generated from the ITS-rRNA gene dataset with TVM + G model. Posterior probabilities more than 65% are given for appropriate clades; bootstrap values greater than 50% are given on appropriate clades in ML analysis. Newly obtained sequences are in underline letters.

33–37 μm, respectively. It differs from *R. troncapitatus* by body length (1383–1856 *vs.* 940–1180 μm), lip region shape (truncate lip region with 7–9 annuli, continuous with body contour *vs.* truncate, with 7–10 annuli and set off from body), and phasmid position (12–24 annuli anterior to level of anus *vs.* varying from four annuli anterior to four posterior to anus).

The *R. brevicaudatus* population from grasses in Brisbane (Australia) was morphologically and morphometrically similar with that analysed in the original description and subsequent reports, as showed by de Man ratios, except for minor differences which may be considered as intraspecific (Colbran, 1962; Van Den Berg and Heyns, 1974). This population was characterised by a slightly shorter body and stylet length than those from the original population from Lawnton, Queensland (533–587 *vs.* 700–800 μm, 21–24 *vs.* 22–27 μm, respectively); but almost identical to a population from South Africa (21–24 *vs.* 19–25 μm, 533–587 *vs.* 500–800 μm, respectively) (Colbran, 1962; Van Den Berg and Heyns, 1974). Similarly, the alpha-numeric codes for *R. brevicaudatus* to be applied to the polytomic identification key for *Rotylenchus* species by Castillo and Vovlas (2005) are coincident with previous descriptions A3–B2–C1–D4–E1–F2–G3–H1–I2–J1–K1.

The *R. buxophilus* population from Napa County (California, USA) agrees fairly well with the original description and the population from Iran, the morphometric of which do not exceed the intraspecific variation reported herein, as showed by de Man ratios and other diagnostic characters (Golden, 1956; Sher, 1965; Geraert and Barooti, 1996).

The *R. pumilus* population from *Urtica* sp. in San Jose park, California (USA) completely fit the original description and data from a French population, except for minor differences which may be considered as intraspecific (Sher, 1961; Germani and Scotto La Massese, 2002). This population was characterised by a slightly larger body and stylet length than those from the original population from Wisconsin, USA (773–906 *vs.* 600–700 μm, 27–31 *vs.* 23–28 μm, respectively) (Sher, 1961); but almost identical in stylet length to a population from France (27–31 *vs.* 26–29 μm, respectively) (Germani and Scotto La Massese, 2002). Similarly, the alpha-numeric codes for *R. pumilus* to be applied to the polytomic identification key for *Rotylenchus* species by Castillo and Vovlas (2005) are coincident with previous descriptions A4–B1–C1–D4–E1–F2–G2–H1–I2–J1–K2.

The *R. robustus* populations from stone pine and grasses in southern Spain and California (USA), respectively, closely agree with the original description and previous reports, showing minor differences which could be considered as intraspecific variations (Sher, 1965; Castillo and Vovlas, 2005). Both populations were clearly differentiated from *R. uniformis* (Thorne, 1949) Loof and Oostenbrink, 1958 by a higher number of lip annuli (6–8 *vs.*

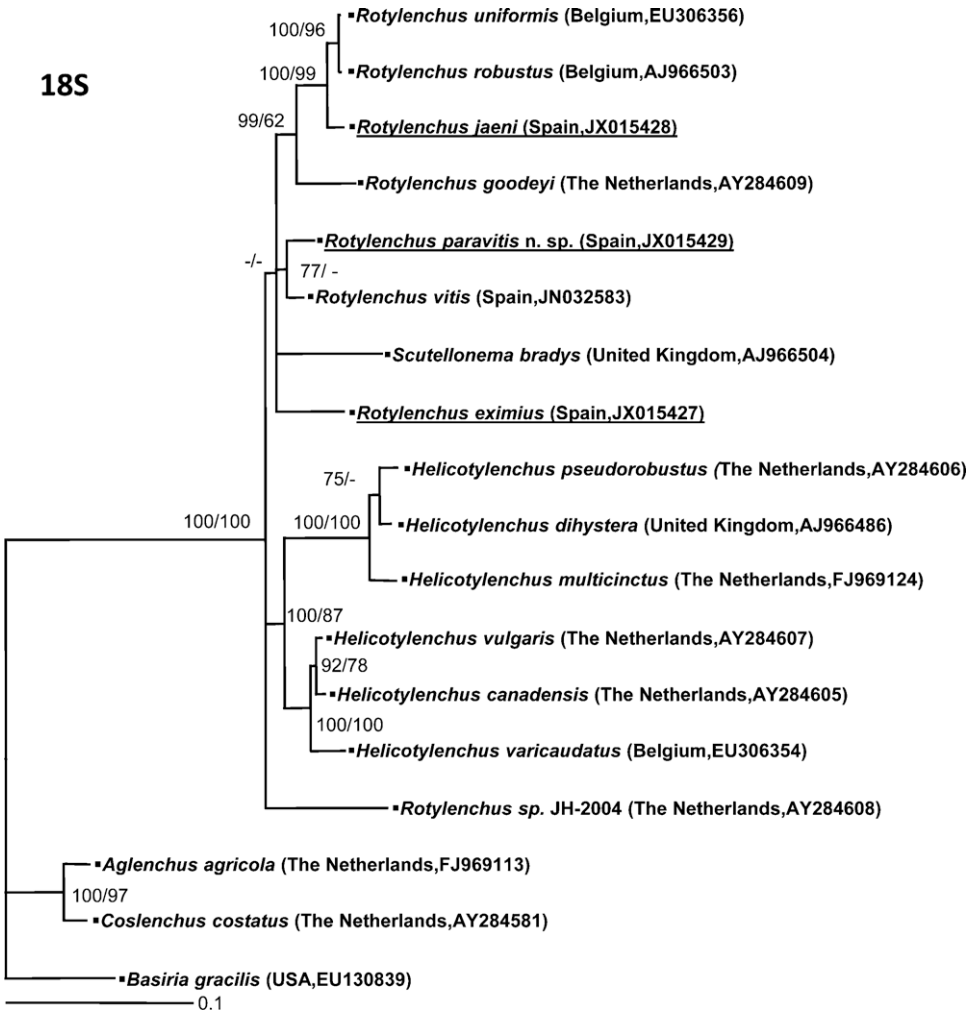

Fig. 11. The 50% majority rule consensus tree from Bayesian analysis generated from the 18S-rRNA gene dataset with TVM1 + I + G model. Posterior probabilities more than 65% are given for appropriate clades; bootstrap values greater than 50% are given on appropriate clades in ML analysis. Newly obtained sequences are in underline letters.

5); lateral fields areolated in pharyngeal region and irregularly areolated at mid-body *vs.* areolated only in pharyngeal region; and female tail hemispherical *vs.* rounded (Castillo and Vovlas, 2005). The alpha-numeric codes for *R. robustus* to be applied to the polytomic identification key for *Rotylenchus* species by Castillo and Vovlas (2005) are coincident with previous descriptions A6–B1–C2–D4–E4–F2–G3–H1–I2–J1–K2. SEM studies for the Spanish and American populations of *R. robustus* showed a similar pattern of lip region, with longitudinal striations in lip annuli, giving a tiled surface appearance (Fig. 8), and were coincident with previous studies (De Grisse et al., 1974; Abrantes et al., 1987).

4.3. Molecular phylogenetic relationships

The phylogenetic relationships inferred in this study based on the D2-D3 of 28S-rRNA and the ITS1 of rRNA gene sequences mostly agrees with well-differentiated lineages obtained in previous studies (Vovlas et al., 2008; Atighi et al., 2011; Cantalapiedra-Navarrete et al., 2012). Nevertheless, small differences may be attributed to additional sequences added in this study. In particular, the position of *R. agnetis* in the present tree differed after including *R. brevicaudatus*, which formed a moderately supported clade with *R. montanus* and with *Rotylenchus* sp. SAS-2006. Phylogeny based on the D2-D3 of 28S-rRNA clearly showed the paraphyly of Hoplolaimidae, which agrees with previous studies (Subbotin et al., 2007; Vovlas et al., 2008; Atighi et al., 2011; Cantalapiedra-Navarrete et al., 2012). This molecular marker separated *Rotylenchus* from other genera within Hoplolaimidae (*i.e. Helicotylenchus*, *Hoplolaimus*, *Scutellonema* and *Aorolaimus*), which agree with the separation by morphological characters, including position of pharyngeal overlapping (dorsal *vs.* ventral), type of phasmid (scutellum-type or pore-like) and stylet knobs (tulip-shaped or rounded). Also, in *Rotylenchus* some lineages derived from molecular markers were congruent with morphological and morphometrical traits for D2-D3 with the major number of species studied, *i.e.* lineage (iii)included species with hemispherical lip regions of 7–8 annuli, long bodies and stylets, but the first one possesses three pharyngeal gland nuclei,; and lineage (iv) grouped two closely related species (*R. vitis* and *R. paravitis* n. sp.) and *R. eximius* sharing only a long stylet and a broadly rounded tail with those species. The ITS1 data set clearly indicated similar relationships and lineages composition with previous studies (Vovlas et al., 2008; Atighi et al., 2011; Cantalapiedra-Navarrete et al., 2012), except for some species, such as *R. vitis* which formed a moderately supported clade with *R. iranicus*, instead of clustering with *R. paravitis* and *R. eximius* which clustered separately or with very low clade support (Figs. 9 and 10). However, these lineages differ between D2D3 and ITS.

The phylogenetic relationships inferred in this study based on the partial *COI* data set was provided for the first time in the genus *Rotylenchus*. Phylogenetic relationships based on the partial *COI* showed similar phylogenies than those detected in D2-D3

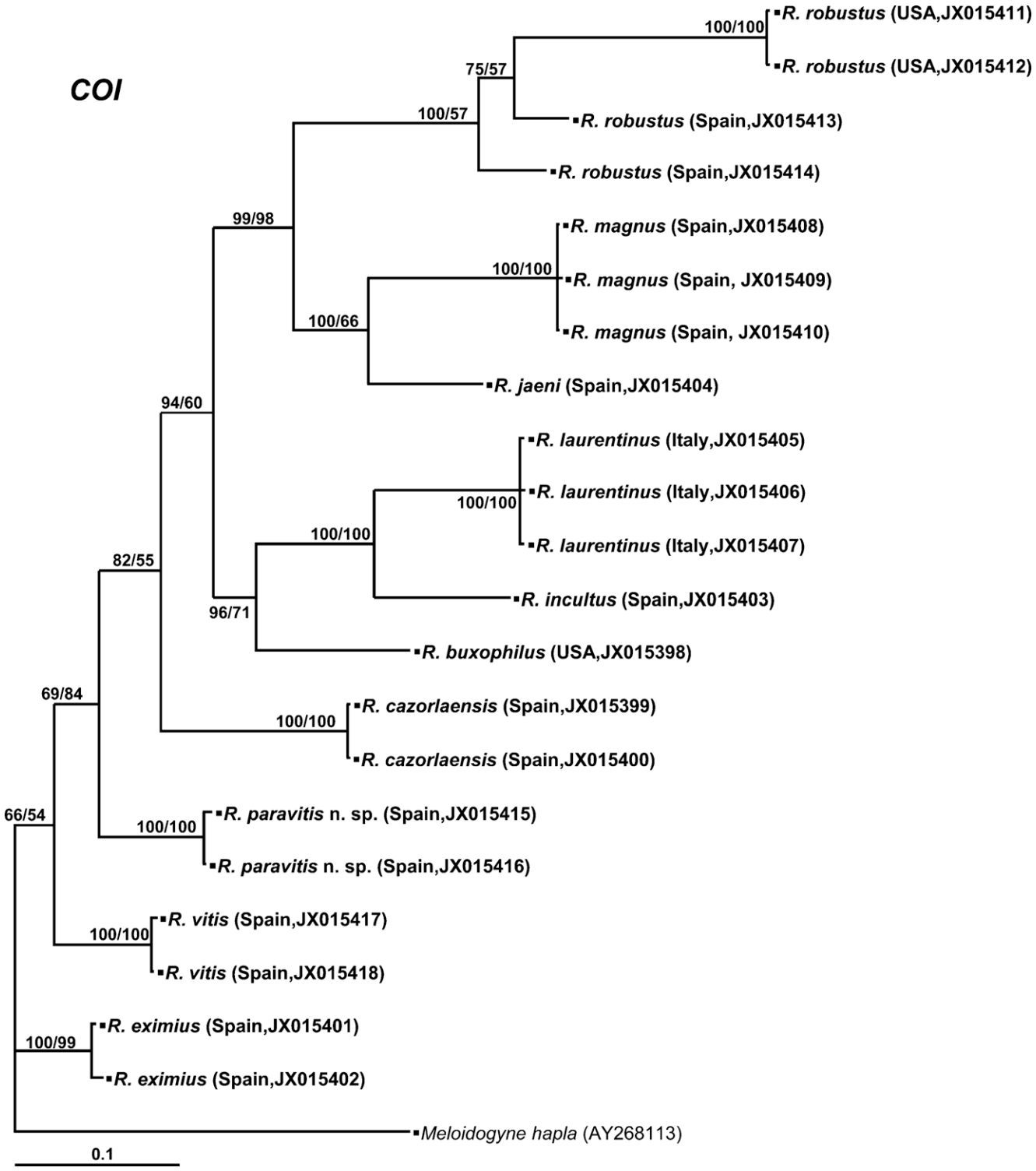

Fig. 12. The 50% majority rule consensus tree from Bayesian analysis generated from the partial *COI* gene dataset with GTR + I + G model. Posterior probabilities more than 65% are given for appropriate clades; bootstrap values greater than 50% are given on appropriate clades in ML analysis. All sequences are newly obtained.

and ITS1 regions for the majority of species. Finally, phylogeny of the available partial 18S sequences suggests a monophyletic relationship within the genus *Rotylenchus*, but additional studies are needed for clarifying this aspect. Molecular markers based on D2-D3 expansion segments of 28S-rRNA and partial 18S did not refute the monophyly of *Rotylenchus* and other genera in the family Hoplolaimidae (*Helicotylenchus* in both markers and *Hoplolaimus* only in D2-D3). However, additional sequences of *Hoplolaimus*, *Scutellonema* and *Aorolaimus* will help in the study of these genera from a phylogenetic point of view. Our results showed that D2-D3 of 28S-rRNA, the ITS1 of rRNA, the partial *COI*, the partial 18S, and partial *hsp90* gen are useful markers for species delimitation. Nevertheless, if the speciation event has taken place recently, the D2-D3 of 28S-rRNA might not be served a good marker to separate *Rotylenchus* spp., as it has been shown for *R. laurentinus* and *R. incultus* (Vovlas et al., 2008). Consequently, phylogenetic

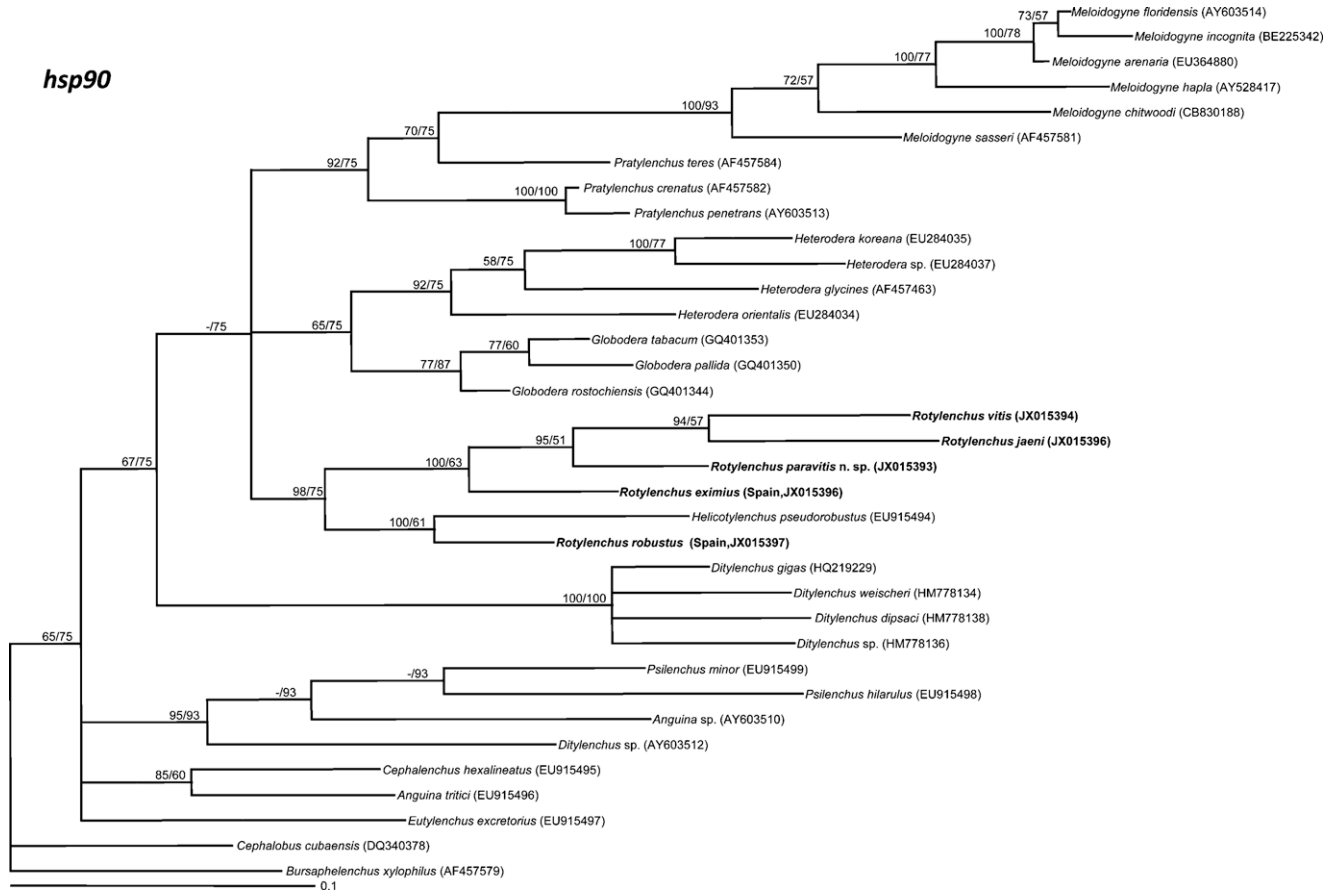

Fig. 13. The 50% majority rule consensus tree from Bayesian analysis generated from the *hsp90* gene dataset with K80 + G model. Posterior probabilities more than 65% are given for appropriate clades; bootstrap values greater than 50% are given on appropriate clades in ML analysis. Newly obtained sequences are in bold letters.

analyses based on the different markers did not result in a general consensus of species grouping, since lineages were maintained for some species (*i.e.* species with hemispherical lip regions of 7–8 annuli, long bodies and stylets), but not in others (*i.e.* position of *R. vitis*, *R. breviannulatus* were quite variable).

Diagnostic PCR-ITS-RFLP profiles with five restriction enzymes, as well as species-specific primer proved to be useful tools for identification of *Rotylenchus* species. Nevertheless, specificity of species specificity of *R. robustus* primers still requires testing with *R. uniformis* samples, and species identity for nematodes previously named as *R. uniformis* by Subbotin et al. (2007) should be confirmed by molecularly comparing with the type materials of this species. There is some controversy on the synonymy of *R. uniformis* with *R. robustus*, since some authors consider both as valid species (Seinhorst and Kuniyasu, 1969; Castillo and Vovlas, 2005) based on differences in six characters including body length, ratio a, dimensions and number of lips annuli, stylet length, and posterior extensions of labial framework, while other authors consider both species as synonyms (Loof and Oostenbrink, 1958; Seinhorst, 1991).

In summary, molecular characterisation and phylogenetic analysis of D2-D3 region ITS1 of rRNA, partial 18S-rRNA, *COI*, and *hsp90* sequences and morphological and morphometric analyses clearly support the proposal of *R. paravitis* n. sp. as a new species. And also, the recognition of this cryptic species within the genus *Rotylenchus* shows that the biodiversity of these nematodes is still not fully understood and need some additional studies. Interestingly, *R. paravitis* n. sp. and *R. vitis* showed clearly different sequences and positions in the phylogenetic analysis, in spite of showing scarce or no differences in morphology or morphometry. Also, RFLP profiles as well as slight minor phenotypic traits suggest speciation between the two taxa. Understanding the range of *R. vitis* and *R. paravitis* n. sp. by new locality reports could help to understand the speciation process in these nematodes.

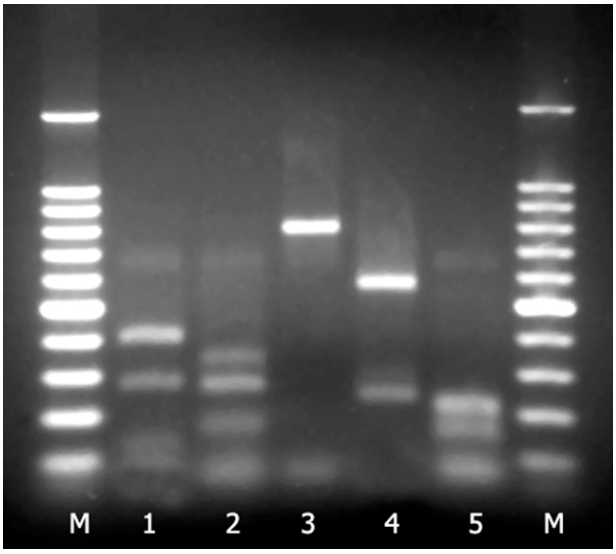

Fig. 14. PCR-D2-D3-28S-RFLP profile for *Rotylenchus paravitis* n. sp. Lines: M – 100 bp DNA ladder (Promega); U – unrestricted PCR product, 1 – *Ava*I, 2 – *Rsa*I, 3 – *Bse*NI, 4 – *Mva*I, 5 – *Hpa*II.

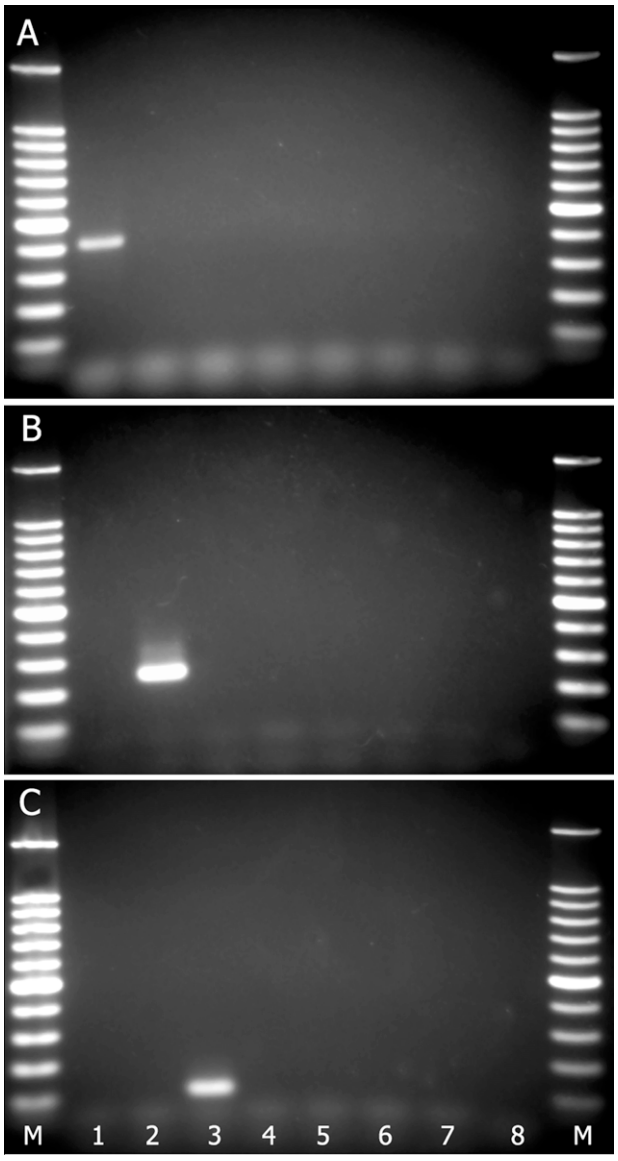

Fig. 15. The gel with specific amplicons obtained in the results of PCR with species specific primers. (A) PCR with the *Rotylenchus robustus* specific primer (TW81 + R_robustus primers). (B) PCR with the *R. vitis* specific primer (TW81 + R_vitis). (C) PCR with the *R. paravitis* n. sp. specific primer (TW81 + R_paravitis). Lanes: M – 100 bp DNA ladder (Promega); 1 – *R. robustus* (CA, USA); 2 – *R. vitis*; 3 – *R. paravitis* n. sp.; 4 – *R. brevicaudatus* (Australia); 5 – *R. buxophilus* (CA, USA); 6 – *R. pumilus* (CA, USA), 7 – *Scutellonema brachyurus* (USA); 8 – control without DNA.

Acknowledgements

This research was supported by grant AGL2009-06955 from 'Ministerio de Ciencia e Innovación' of Spain, grant AGR-136 from 'Consejería de Economía, Innvovación y Ciencia' from Junta de Andalucía, and the European Social Fund. The authors thank J. Martín-Barbarroja, and G. León-Ropero from IAS-CSIC for excellent technical assistance, M. Pedram (Tarbiat Modares University, Tehran, Iran) for his help with line drawing, and B. Landa (IAS-CSIC) for critical reading of the manuscript.

References

Abolafia, J., Liebanas, G., Peña-Santiago, R., 2002. Nematodes of the order Rhabditida from Andalucía Oriental, Spain. The subgenus *Pseudacrobeles* Steiner, 1938, with description of a new species. Journal of Nematode Morphology and Systematics 4, 137–154.

Abrantes, I.M.d.O., Vovlas, N., Santos, M.S.N., 1987. Morphological studies on six tylenchid nematode species associated with olive in Portugal. Ciencia Biologica. Ecology and Systematics 7, 1–9.

Andrássy, I., 1958. *Hoplolaimus tylenchiformis* Daday, 1905 (Syn, *H. coronatus* Cobb, 1923) und die Gattungen der Unterfamilie Hoplolaiminae Filipjev, 1936. Nematologica 3, 44–56.

Atighi, M.R., Pourjam, E., Pedram, M., Cantalapiedra-Navarrete, C., Palomares-Rius, J.E., Castillo, P., 2011. Molecular and morphological characterisations of two new *Rotylenchus* species from Iran. Nematology 13, 951–964.

Baydulova, L.A., 1984. A new species from the genus *Rotylenchus* (Nematoda: Hoplolaimidae) from the northern pre-Caspian region. Byulletin' Vsesoyuznogo Instituta Gel' mintologii im. K. I. Skryabina 36, 67–68.

Boutsika, K., Brown, D.J.F., Phillips, M.S., Blok, V.C., 2004. Molecular characterisation of the ribosomal DNA of *Paratrichodorus macrostylus*, *P. pachydermus*, *Trichodorus primitivus* and *T. similis* (Nematoda: Trichodoridae). Nematology 6, 641–654.

Cantalapiedra-Navarrete, C., Liébanas, G., Archidona-Yuste, A., Palomares-Rius, J.E., Castillo, P., 2012. Molecular and morphological characterisation of *Rotylenchus vitis* n. sp. (Nematoda: Hoplolaimidae) infecting grapevine in southern Spain. Nematology 14, 235–247.

Castillo, P., Gómez Barcina, A., 1987. *Rotylenchus cazorlaensis* sp. n. and new record of *R. fallorobustus* Sher, 1965 (Nematoda: Tylenchida) from south-eastern Spain. Nematologica 33, 393–400.

Castillo, P., Vovlas, N., 2005. *Bionomics and identification of the genus* Rotylenchus (*Nematoda*: *Hoplolaimidae*). In: Hunt, D.J., Perry, R.N. (series editors), Nematology Monographs and Perspectives, vol. 3. Brill Academic Publishers, Leiden, The Netherlands, 377 pp.

Castillo, P., Vovlas, N., Subbotin, S., Troccoli, A., 2003. A new root-knot nematode, *Meloidogyne baetica* n. sp. (Nematoda: Heteroderidae), parasitizing wild olive in Southern Spain. Phytopathology 93, 1093–1102.

Colbran, R.C., 1962. Studies of plant and soil nematodes. 5. Four new species of Tylenchoidea from Queensland Pineapple Fields. Queens. Journal of Agricultural Science 19, 231–239.

Coolen, W.A., 1979. Methods for extraction of *Meloidogyne* spp. and other nematodes from roots and soil. In: Lamberti, F., Taylor, C.E. (Eds.), Root-knot Nematodes (Meloidogyne species). Systematics, Biology and Control. Academic Press, New York, pp. 317–329.

Curran, J., Driver, F., Ballard, J.W.O., Milner, R.J., 1994. Phylogeny of *Metarhizium*: analysis of ribosomal DNA sequence data. Mycological Research 98, 547–555.

De Grisse, A.T., 1969. Redescription ou modifications de quelques techniques utilisées dans l'étude des nématodes phytoparasitaires. Mededelingen van de Faculteit Landbouwwetenschappen Rijksuniversiteit Gent 34, 351–369.

De Grisse, A.T., Lippens, P.L., Coomans, A., 1974. The cephalic sensory system of *Rotylenchus robustus* and a comparison with some other Tylenchids. Nematologica 20, 88–95.

de Man, J.G., 1876. Onderzoekingen over vrij in de aarde levende Nematoden. Tijdschrift voor Nederlands Dierkunde Vereen 2, 78–196.

Derycke, S., Vanaverbeke, J., Rigaux, A., Backeljau, T., Moens, T., 2010. Exploring the use of cytochrome oxidase c subunit 1 (*COI*) for DNA barcoding of free-living marine nematodes. PLoS ONE 5 (10), e13716, http://dx.doi.org/10.1371/journal.pone.0013716.

Eroshenko, A.S., 1981. Phytopathogenic nematodes of forest undergrowth of the families Tylenchorhynchidae and Hoplolaimidae (Nematoda). In: Eroshenko, A.C., Belogurov, O.I. (Eds.), Freeliving and Plant-Parasitic Nematodes in the Far-East. Vladivostok. Dal'nev. Nauch. Tsentr Akad. Nauk SSR, pp. 22–27, 85–92.

Filipjev, I.N., 1934. The classification of free-living nematodes and their relations to parasitic nematodes. Smithsonian Miscellaneous Collections 89, 1–63.

Filipjev, I.N., 1936. On the classification of the Tylenchinae. Proceedings of the Helminthological Society of Washington 3, 80–82.

Fortuner, R., 1987. A reappraisal of Tylenchina (Nemata). 8. The family Hoplolaimidae Filip'jev, 1934. Review de Nématologie 10, 219–232.

Geraert, E., Barooti, S., 1996. Four *Rotylenchus* from Iran, with a key to the species. Nematologica 42, 503–520.

Germani, G., Scotto La Massese, C., 2002. Description of four new species and two populations of *Rotylenchus* (Nematoda: Hoplolaimidae). Nematologia Mediterranea 30, 203–208.

Golden, A.M., 1956. Taxonomy of the spiral nematodes (*Rotylenchus* and *Helicotylenchus*), and the developmental stages and host-parasite relationships of *R. buxophilus*, n. sp., attacking boxwood. Bulletin A-85, University of Maryland, MD, USA, Agricultural Experimental Station, 28 pp.

Gutiérrez-Gutiérrez, C., Palomares-Rius, J.E., Cantalapiedra-Navarrete, C., Landa, B.B., Esmenjaud, D., Castillo, P., 2010. Molecular analysis and comparative morphology to resolve a complex of cryptic *Xiphinema* species. Zoologica Scripta 39, 483–498.

Gutiérrez-Gutiérrez, C., Castillo, P., Cantalapiedra-Navarrete, C., Landa, B.B., Derycke, S., Palomares-Rius, J.E., 2011. Genetic structure of *Xiphinema pachtaicum* and *X. index* populations based on mitochondrial DNA variation. Phytopathology 101, 1168–1175.

Hall, T.A., 1999. BioEdit: a user-friendly biological sequence alignment editor and analysis program for windows 95/98/NT. Nucleic Acids Symposium Series 41, 95–98.

Huelsenbeck, J.P., Ronquist, F., 2001. MrBAYES: Bayesian inference of phylogenetic trees. Bioinformatics 17, 754–755.

Hugall, A., Moritz, C., Stanton, J., Wolstenholme, D.R., 1994. Low, but strongly structured mitochondrial DNA diversity in root knot nematodes (*Meloidogyne*). Genetics 136, 903–912.

Khan, M.L., Khan, S.H., 1982. Three new species of genus *Orientylus* Jairajpuri & Siddiqi, 1977 associated with fruit trees in India (Rotylenchoidinae: Nematoda). Indian Journal of Nematology 12, 111–117.

Linford, M.B., Oliveira, J.M., 1940. *Rotylenchulus reniformis*, nov. gen., n. sp., a nematode parasite of roots. Proceedings of the Helminthological Society of Washington 7, 35–42.

Loof, P.A.A., Oostenbrink, M., 1958. Die identitat van *Tylenchus robustus* de Man. Nematologica 3, 34–43.

Madani, M., Ward, L., De Boer, S., 2011. *Hsp90* gene, an additional target for discrimination between the potato cyst nematodes, *Globodera rostochiensis*, *G. pallida*, and the related species *G. tabacum tabacum*. European Journal of Plant Pathology 130, 271–285.

Page, R.D.M., 1996. TREEVIEW: an application to display phylogenetic trees on personal computers. Computer Applications in the Biosciences 12, 357–358.

Palomares-Rius, J.E., Castillo, P., Liébanas, G., Vovlas, N., Landa, B.B., Navas-Cortés, J.A., Subbotin, S.A., 2010. Description of *Pratylenchus hispaniensis* n. sp. from Spain and considerations on the phylogenetic relationship among selected genera in the family Pratylenchidae. Nematology 12, 429–451.

Perry, V.G., Darling, H.M., Thorne, G., 1959. Anatomy, taxonomy, and control of certain spiral nematodes attacking blue grass in Wisconsin. University of Wisconsin Research Bulletin 207, 1–24.

Posada, D., 2008. jModelTest: phylogenetic model averaging. Molecular Biology and Evolution 25, 1253–1256.

Scognamiglio, A., Talamé, M., 1972. *Rotylenchus laurentinus* n. sp. (Nematoda: Hoplolaimidae). Bollettino del Laboratorio di Entomologia Agraria Filippo Silvestri 30, 1–7.

Scotto La Massèse, C., Germani, G., 1998. Description of two new species of *Rotylenchus* and two populations of *R. agnetis*. Nematologica 44, 37–44.

Seinhorst, J.W., 1991. The identity of *Tylenchus robustus* de Man, 1876, with a remark on distortions in de Man's (1876) figures. Nematologica 37, 119–122.

Seinhorst, J.W., Kuniyasu, K., 1969. *Rotylenchus uniformis* (Thorne) on carrots. Netherlands Journal of Plant Pathology 75, 205–223.

Sher, S.A., 1961. Revision of the Hoplolaiminae (Nematoda). I. Classification of nominal genera and nominal species. Nematologica 6, 155–169.

Sher, S.A., 1965. Revision of the Hoplolaiminae (Nematoda). V. *Rotylenchus* Filipjev, 1936. Nematologica 6, 173–198.

Siddiqi, M.R., 2000. Tylenchida Parasites of Plants and Insects, 2nd edition. CABI Publishing, Wallingford, UK, 833 pp.

Skantar, A.M., Carta, L.K., 2004. Molecular characterization and phylogenetic evaluation of the *hsp90* gene from selected nematodes. Journal of Nematology 36, 466–480.

Steiner, G., 1945. *Helicotylenchus*, a new genus of plant-parasitic nematodes and its relationship to *Rotylenchus* Filipjev. Proceedings of the Helminthological Society of Washington 12, 34–38.

Subbotin, S.A., Sturhan, D., Chizhov, V.N., Vovlas, N., Baldwin, J.G., 2006. Phylogenetic analysis of Tylenchida Thorne, 1949 as inferred from D2 and D3 expansion fragments of the 28S rRNA gene sequences. Nematology 8, 455–474.

Subbotin, S.A., Sturhan, D., Rumpenhorst, H.J., Moens, M., 2003. Molecular and morphological characterisation of the *Heterodera avenae* complex species (Tylenchida: Heteroderidae). Nematology 5, 515–538.

Subbotin, S.A., Moens, M., 2006. Molecular taxonomy and phylogeny. In: Perry, R., Moens, M. (Eds.), Plant Nematology. CABI, Wallingford, UK, pp. 33–58.

Subbotin, S.A., Sturhan, D., Vovlas, N., Castillo, P., Tanyi Tambe, J., Moens, M., Baldwin, J.G., 2007. Application of the secondary structure model of rRNA for phylogeny: D2-D3 expansion segments of the LSU gene of plant-parasitic nematodes from the family Hoplolaimidae Filipjev, 1934. Molecular Phylogenetics and Evolution 43, 881–890.

Swofford, D.L., 2003. PAUP*: Phylogenetic Analysis Using Parsimony (*and other methods), Version 4.0b 10. Sinauer Associates, Sunderland, MA.

Tanha Maafi, Z., Subbotin, S.A., Moens, M., 2003. Molecular identification of cyst-forming nematodes (Heteroderidae) from Iran and a phylogeny based on ITS-rDNA sequences. Nematology 5, 99–111.

Thompson, J.D., Gibson, T.J., Plewniak, F., Jeanmougin, F., Higgins, D.G., 1997. The CLUSTAL_X windows interface: flexible strategies for multiple sequence alignment aided by quality analysis tools. Nucleic Acids Research 25, 4876–4882.

Thorne, G., 1949. On the classification of the *Tylenchida*, new order (Nematoda, Phasmidia). Proceedings of the Helminthological Society of Washington 16, 37–73.

Van Den Berg, E., Heyns, J., 1974. South African Hoplolaiminae. 3. The genus *Rotylenchus* Filipjev, 1936. Phytophylactica 6, 165–184.

von Daday, E., 1905. Untersuchungen über die Süsswasser-Mikrofauna Paraguays. Miteinem Anhang von W. Michaelsen. Zoologica (Stuttgart) 18, 1–349, 362–374.

Vovlas, N., Subbotin, S.A., Troccoli, A., Liébanas, G., Castillo, P., 2008. Description of *Rotylenchus montanus* sp. n. and recognition of *R. jaeni* comb. n. as a separate species with approaches to molecular phylogeny of the genus *Rotylenchus* (Nematoda, Tylenchida). Zoologica Scripta 37, 521–537.

Wouts, W.M., Sturhan, D., 1999. Descriptions of *Rotylenchus* species from New Zealand, including *R. labiodiscus* sp. n. (Nematoda: Hoplolaimidae). New Zealand Journal of Zoology 26, 395–404.

Zancada, M.C., 1985. *Rotylenchus magnus* sp. n. and *R. mesorobustus* sp. n. (Nematoda: Tylenchida) from Spain. Nematologica 31, 134–142.